PLOS ONE

RESEARCH ARTICLE

Comprehensive genomic analysis reveals virulence factors and antibiotic resistance genes in *Pantoea agglomerans* KM1, a potential opportunistic pathogen

Robin B. Guevarra[1], Stefan Magez[1,2,3], Eveline Peeters[4], Mi Sook Chung[5], Kyung Hyun Kim[6], Magdalena Radwanska[1,7]*

1 Laboratory for Biomedical Research, Department of Environmental Technology, Food Technology and Molecular Biotechnology, Ghent University Global Campus, Incheon, Republic of Korea, **2** Department of Biochemistry and Microbiology, Ghent University, Ghent, Belgium, **3** Laboratory of Cellular and Molecular Immunology, Vrije Universiteit Brussel, Brussels, Belgium, **4** Research Group of Microbiology, Vrije Universiteit Brussel, Brussels, Belgium, **5** Department of Food and Nutrition, Duksung Women's University, Dobong-gu, Seoul, Republic of Korea, **6** Department of Biotechnology & Bioinformatics, Korea University, Sejong, Republic of Korea, **7** Department of Biomedical Molecular Biology, Ghent University, Ghent, Belgium

* magdalena.radwanska@ghent.ac.kr

Citation: Guevarra RB, Magez S, Peeters E, Chung MS, Kim KH, Radwanska M (2021) Comprehensive genomic analysis reveals virulence factors and antibiotic resistance genes in *Pantoea agglomerans* KM1, a potential opportunistic pathogen. PLoS ONE 16(1): e0239792. https://doi.org/10.1371/journal.pone.0239792

Editor: Feng Gao, Tianjin University, CHINA

Received: September 11, 2020

Accepted: November 29, 2020

Published: January 6, 2021

Data Availability Statement: The raw sequence data were deposited to the NCBI SRA database (accession number SRR11347418). The BioProject accession number for this project is PRJNA613157.

Funding: This work was supported by the Ghent University Global Campus (GUGC) core laboratory funding. The funders had no role in study design, data collection and analysis, decision to publish, or preparation of the manuscript.

Abstract

Pantoea agglomerans is a Gram-negative facultative anaerobic bacillus causing a wide range of opportunistic infections in humans including septicemia, pneumonia, septic arthritis, wound infections and meningitis. To date, the determinants of virulence, antibiotic resistance, metabolic features conferring survival and host-associated pathogenic potential of this bacterium remain largely underexplored. In this study, we sequenced and assembled the whole-genome of *P. agglomerans* KM1 isolated from kimchi in South Korea. The genome contained one circular chromosome of 4,039,945 bp, 3 mega plasmids, and 2 prophages. The phage-derived genes encoded integrase, lysozyme and terminase. Six CRISPR loci were identified within the bacterial chromosome. Further in-depth analysis showed that the genome contained 13 antibiotic resistance genes conferring resistance to clinically important antibiotics such as penicillin G, bacitracin, rifampicin, vancomycin, and fosfomycin. Genes involved in adaptations to environmental stress were also identified which included factors providing resistance to osmotic lysis, oxidative stress, as well as heat and cold shock. The genomic analysis of virulence factors led to identification of a type VI secretion system, hemolysin, filamentous hemagglutinin, and genes involved in iron uptake and sequestration. Finally, the data provided here show that, the KM1 isolate exerted strong immunostimulatory properties on RAW 264.7 macrophages *in vitro*. Stimulated cells produced Nitric Oxide (NO) and pro-inflammatory cytokines TNF-α, IL-6 and the anti-inflammatory cytokine IL-10. The upstream signaling for production of TNF-α, IL-6, IL-10, and NO depended on TLR4 and TLR1/2. While production of TNF-α, IL-6 and NO involved solely activation of the NF-κB, IL-10 secretion was largely dependent on NF-κB and to a lesser extent on MAPK Kinases. Taken together, the analysis of the whole-genome and immunostimulatory properties provided in-depth characterization of the *P. agglomerans* KM1 isolate

Competing interests: The authors have declared that no competing interests exist.

shedding a new light on determinants of virulence that drive its interactions with the environment, other microorganisms and eukaryotic hosts

Introduction

Kimchi is a well-known Korean vegetable side dish prepared based on a fermentation process conducted by lactic acid bacteria (LAB) [1, 2]. Often homemade, kimchi is traditionally considered as a functional food with potential health benefits including anti-cancer, anti-obesity, anti-oxidant and anti-aging properties [1]. The fermentation process of a Korean Baechu cabbage leads to a steadily decreasing pH, reaching 4.5 after approximately one month of fermentation. This process is followed by the subsequent growth of the LAB and elimination of potentially pathogenic bacterial species that are sensitive to low pH [3]. Recently, the interest in consumption of kimchi has increased, leading to a global distribution of this traditional Korean side dish. However, the time needed for a complete fermentation to take place is often reduced in favor of a 'better' taste, resulting in frequent consumption of a 'short-term'fermented kimchi. This, in turn, poses potential health risks documented by previous publications that reported several outbreaks associated with a foodborne pathogen-contaminated kimchi [4, 5]. It was shown that pathogenic *Escherichia coli* and *Salmonella* can survive in kimchi during fermentation, suggesting that the risk for contamination of kimchi with pathogens, in both commercial and homemade preparations, should not be underestimated [6].

Pantoea agglomerans (formerly *Enterobacter agglomerans* and *Erwinia herbicola*) is a Gram-negative member of the Enterobacteriaceae family that is ubiquitous in nature and is found in a wide variety of environments. *P. agglomerans* grows as an epiphyte on plants [7], exists in soil [8], insects [9] various food sources [10] and has been found in clinical samples including pus, sputum, urine, bloodstream, tracheal and joint aspirate, and it has also been identified as a significant plant pathogen [11–14]. Different strains of *P. agglomerans* exert beneficial antibacterial activity against phytopathogens [15], which make them an attractive biocontrol agent [16] as well as a plant growth promoter [17]. While *P. agglomerans* strains E325 and P10c biocontrol agents are allowed for agricultural use in several countries, including the USA and New Zealand, it remains to be approved for commercial purposes by the European countries [18]. The lipopolysaccharide (LPS) extracted from *P. agglomerans* is a potent adjuvant in mucosal vaccinations, triggering production of IgGs and IgAs, and inducting TNF-α and IL-6 secretion through activation of a Toll-like receptor 4 (TLR4) [19]. *P. agglomerans* derived LPS has anti-cancer properties in B16 melanoma model in mice [20], and an oral administration of this molecule contributed to prevention of atherosclerosis and hypertension [21].

While *P. agglomerans* may exert some beneficial roles, it can cause life-threatening infections in immunosuppressed individuals, elderly, newborns and infants [12, 22, 23]. For example, clinical isolates containing *P. agglomerans* can cause a wide range of infections such as neonatal sepsis [24], joint infection [11], pneumonia and meningitis [25]. *P. agglomerans* furthermore poses health risks for adults, being responsible for occupational respiratory diseases of workers exposed to dust in factories processing cotton, herbs, grain, wood, and tobacco [22, 26, 27]. Affected individuals suffered from inflammation of the respiratory system and allergic pulmonary disorders [23]. In animal studies, inhaled nanoparticles carrying *P. agglomerans* LPS induced airway inflammation with alveolar macrophages secreting pro-inflammatory cytokines and superoxide anion [28]. Other studies conducted using experimental mouse models showed that ingested *P. agglomerans* was able to colonize the gut, cross the gut barrier

to the bloodstream, and cause systemic dissemination to various organs [29]. Taken together, a number of reports demonstrate the ambiguous nature of *P. agglomerans* in relation to possible beneficial or detrimental effects on health. In this context, there is scarce information about possible determinants of virulence leading to pathology of *P. agglomerans* associated diseases.

Advances in genome sequencing allowed for identification of virulence factors, and plant growth promoting determinants in genomes of various species belonging to genus *Pantoea* [7, 17, 30]. In plants, some of the isolated pathogenic stains of *P. agglomerans* are known to cause gall-formation, which contained type III secretion system (T3SS) and its effectors through acquisition of pathogenicity plasmid (pPATH). *P. agglomerans* biopesticide properties are related to the presence of genes encoding antibiotics such as pantocins, herbicolins, microcins, and phenazines, which target for example amino acid biosynthesis genes in *Erwinia amylovora*, the causative agent of fire blight [14].

While most *P. agglomerans* genome studies focused on plant isolates, the determinants of virulence present in clinical isolates remain largely undiscovered. Our current study aimed at helping to close this knowledge gap, based on the analysis of the sequenced genome and tested immuno-properties of the isolated foodborne *P. agglomerans* KM1 strain. We identified genes involved in virulence, antibiotic resistance, adaptations to stress and interactions with other microorganisms and eukaryotic hosts. The study also demonstrated immuno-modulatory properties of *P. agglomerans* KM1 and mechanisms involved in secretion of pro-inflammatory and anti-inflammatory cytokines by macrophages.

Materials and methods

Isolation and growth conditions

P. agglomerans KM1 was isolated from short-term fermented homemade kimchi pH 4.5. All isolation procedures were conducted in sterile conditions. Blended kimchi leaves and juice samples were filtered through sterile gauze and spun down for 15 seconds to recover liquid fractions. These were plated out onto Luria Bertani (LB) agar plate and incubated overnight at 37˚C. From the kimchi juice and leaves, eight and nineteen glistening yellow-pigmented colonies were counted on the 10^{-4} diluted sample, respectively.

Genomic DNA extraction and 16S rRNA based identification

A single colony of *P. agglomerans* KM1 was grown in LB broth (Conda, Spain) overnight at 37˚C. The genomic DNA was isolated using the LaboPass™ Tissue Genomic DNA mini kit (Cosmo Genetech, Seoul, South Korea) according to the manufacturer's protocol. The identity of the isolate was verified through 16S rRNA gene sequencing. The 16S rRNA gene was amplified from the extracted genomic DNA using 16S universal primers 27F (`5′-AGA GTTTG ATCMTGGCTCAG-3′`) and 1492R (`5′-GGTTACCTTGTTACGACTTC-3′`) and sequenced using an automated ABI3730XL capillary DNA sequencer (Applied Biosystems, USA) for taxonomic identification at Cosmo Genetech (Seoul, South Korea). The 16S rRNA sequences were confirmed through BLASTn search against the NCBI microbial 16S database.

Genome sequencing and assembly

The genome of *P. agglomerans* KM1 was sequenced using the Illumina HiSeq 4000 and 2 × 150 bp with an insert size of 350 bp at Macrogen, Inc. (Seoul, South Korea). Libraries were generated from1 μg of genomic DNA using the TruSeq® DNA PCR-free Library Prep Kit (Illumina) according to the manufacturer's protocol. The quality control of the raw reads was

performed using FASTQC v.0.11.9, and quality trimming was done based on FASTQC report using Trimmomatic v.0.39. Obtained quality trimmed reads were used for *de novo* assembly using SPAdes v3.14.1 [31] with default parameters. The final genome assembly was polished with the Illumina reads using Pilon v.1.23 [32]. Bandage software (v.0.8.1) was used to detect and extract the sequences of circular plasmid assemblies [33]. The sequences of these assemblies were screened for the presence of potential plasmids by aligning the sequences against the NCBI nucleotide database using BLASTn. The quality of the genome assembly was evaluated using QUAST v5.0.2 [34], and the assessment of the genome completeness was performed using BUSCO v4.0.5 [35]. The resulting contigs were reordered using the Mauve Contig Mover algorithm in Mauve v2.4.0 against the closest complete genome of *Pantoea agglomerans* C410P1 as a reference (GenBank accession number CP016889). The whole-genome shotgun project of *P. agglomerans* KM1 was deposited at NCBI GenBank under accession number NZ_JAAVXI000000000.

Genome annotation

Functional genome annotation of *P. agglomerans* KM1 was conducted using NCBI Prokaryotic Genome Annotation Pipeline (PGAP) [36]. The tRNA genes were identified by tRNAscan-SE v.2.0 [37] and rRNA genes with RNAmmer v.1.2 [38]. The Cluster of Orthologous Groups (COG) functional annotation was performed using RPS-BLAST program against the COG database within the WebMGA server [39]. For Subsystem functional categorization, SEED annotation was used with the SEED viewer within the Rapid Annotations and applying Subsystems Technology (RAST) server v2.0 [40]. The circular genome maps were generated using the GView v1.7 [41].

Phylogenetic analysis

Phylogenetic trees were constructed based on the average nucleotide identity (ANI) values, and using multilocus sequence analysis (MLSA). The overall similarity between the whole-genome sequences was calculated using the Orthologous Average Nucleotide Identity Tool (OAT) v0.93.1 [42]. Phylogenetic tree was constructed based on the concatenated sequences of the six protein-coding genes *fusA*, *gyrB*, *leuS*, *pyrG*, *rplB*, and *rpoB* [43] using the Molecular Evolutionary Genetic Analysis X (MEGA X) software using the neighbor-joining method with 1,000 randomly selected bootstrap replicates [44]. The NCBI GenBank assembly accession numbers of the *Pantoea* genomes used for phylogenetic analysis are the following: *P. agglomerans* KM1 (GCA_012241415.1), *P. agglomerans* C410P1 (GCA_001709315.1), *P. agglomerans* UAEU18 (GCA_010523255.1), *P. agglomerans* Tx10 (GCA_000475055.1), *P. agglomerans* IG1 (GCA_000241285.2), *P. agglomerans* JM1 (GCA_002222515.1), *P. agglomerans* TH81 (GCA_010523255.1), *P. agglomerans* L15 (GCA_003860325.1), *P. vagans* MP7 (GCA_000757435.1), *P. vagans* C9-1 (GCA_000148935.1), *P. stewartii* subsp. *stewartii* DC283 (GCA_002082215.1), *P. ananatis* LMG 20103 (GCA_000025405.2), *P. ananatis* LMG 2665^{T} (GCA_000661975.1) and *Escherichia coli* strain K12 substr. MG1655 (GCA_000005845.2).

Comparative genomics

The genome synteny analysis was performed using the progressive Mauve algorithm in Mauve v2.3.0 [45] to visualize the genome alignments of the *P. agglomerans* KM1 draft genome with *P. agglomerans* C410P1 as a reference (GenBank accession number CP016889). The Mauve software was used to predict chromosomal rearrangement such as insertion, inversion and translocation. The pan-genome analysis was conducted using the retrieved published *P. agglomerans* complete genomes in the NCBI database including those of C410P1

(GCA_001709315.1), UAEU18 (GCA_010523255.1), TH81 (GCA_003704305.1), and L15 (GCA_003860325.1). Prior to pan-genome analysis, Rapid Prokaryotic Genome Annotation (PROKKA) [46] pipeline was used to annotate the genome sequences with Roary software [47] to create the pan-genome and using the Gview Server for visualization [41].

Prediction of genomic islands, prophages and CRISPRs

Identification and visualization of putative genomic islands were conducted using IslandPick, IslandPath-DIMOB, and SIGI-HMM prediction methods in IslandViewer4 [48]. Prophages were identified using PHAge Search Tool Enhanced Release (PHASTER) [49]. CRISPRFinder software was used to identify clustered regularly interspaced short palindromic repeats (CRISPRs) [50].

Biochemical characterization

The isolate was tested for presence of a cytochrome oxidase using the 70439 Oxidase assay (Sigma-Aldrich, MO, USA) according to instruction provided by the manufacturer. The presence of a catalase activity was assessed by exposure of a bacterial colony to 3% hydrogen peroxide (Daeyung, Gyeonggi-do, South Korea). Further biochemical characterization was performed using the Analytical Profile Index (API) 20E test (BioMérieux, France) according to manufacturer's protocol. The index profile was determined with the online API 20E v5.0 identification software (apiweb.biomerieux.com).

Antibiotic resistance gene identification and susceptibility testing

Antibiotic resistance genes (ARGs) were predicted using the BLASTn method against the Comprehensive Antibiotic Resistance Database (CARD) [51] using an identity cut-off of 70% and an E-value $< 1.0\ E^{-6}$. Antibiotic susceptibility test was done using the Kirby-Bauer disk diffusion method on Mueller Hinton agar according to the Clinical and Laboratory Standards Institute (CLSI). Commercially prepared antibiotic disks used in this study were kanamycin (30 μg), streptomycin (10 μg), imipenem (10 μg), vancomycin (10 μg), ofloxacin (5 μg), ampicillin (30 μg), penicillin G (10 iu), rifampicin (5 μg), bacitracin (10 μg), fosfomycin (50 μg), and chloramphenicol (30 μg) (Thermo Fisher Scientific, MA, USA).

Identification of virulence factors

The virulence factors encoding genes of *P. agglomerans* KM1 were investigated using the BLASTn method against the virulence factor database (VFDB) [52] with an identity cut-off of 80%. For virulence gene identification against the VFDB, an E-value $<1.0\ E^{-6}$ was set for BLAST searches. The identified hallmarks of type VI secretion system effectors, the *Hcp* and *VgrG* genes, were validated using polymerase chain reaction with the following primers: Hcp-F: `TGTAAACCAGCGCCATCAGT`; Hcp-R: `ACCGGTAATGCACAGCTGAA`; VgrG-F: `TGAATCCGCTTGCTTCCTGT`; VgrG-R: `ATATCGCCCATGCGTTCCAT`. The primers used in the study were designed using NCBI Primer-BLAST. The thermal cycling conditions consisted of an initial denaturation at 95˚C for 5 min, followed by 25 cycles of denaturation at 95˚C for 30 sec, annealing at 55˚C for 30 sec, and elongation at 72˚C for 2 min, with a final extension at 72˚C for 10 min. The PCR products were gel purified and sequenced using an ABI3730XL machine (Applied Biosystems, USA) at Cosmo Genetech (Seoul, South Korea). The sequences were identified using BLASTx program.

Immuno-stimulations and inhibition studies

A heat-inactivated stock of *P. agglomerans* KM1 was prepared by first growing a bacterial culture in LB medium to an optical density of 0.9, measured at 600 nm. Bacterial cells subsequently were spun down for 5 min and re-suspended in 1 ml of a sterile and endotoxin free Dulbecco's PBS (Welgene, Gyeongsangbuk-do, South Korea) at a concentration of 10^8/ml, and were heat inactivated for 3 hours at 65˚C. These cells were used to stimulate murine macrophage RAW 264.7 cell line (ATCC TIB 71, American Type Culture Collection, VA, USA) *in vitro*. The RAW 264.7 macrophages were grown in High glucose Dulbecco's Modified Eagle Medium (DMEM, Capricorn Scientific, Germany) supplemented with 10% heat-inactivated fetal bovine serum (Atlas Biologicals, CO, USA), 100 U.mL-1 Penicillin, and 100 μg.mL-1 Streptomycin (Capricorn Scientific, Germany). One ml cultures of 10^6 RAW 264.7 cells were stimulated with 10^6 heat-inactivated *P. agglomerans* or 1 ug/ml of the *E. coli* LPS-EK Ultrapure (Invivogen, CA, USA). This commercial LPS preparation was shown to activate only the TLR4 signaling. The stimulated cells were incubated for 24 hr at 37˚C, afterwards culture supernatants were collected and stored at -20˚C for cytokine ELISA. For inhibition studies of immunostimulatory properties of *P. agglomerans* different inhibitors of intracellular pathways were used. The involvement of the NF-κB was tested using irreversible inhibitor Bay 11–7082 at 10 μM (Invivogen, CA, USA). The action of MAPK Kinases (MEK1 and MEK2) was blocked by the use of a selective inhibitor UO126 at 5 μM (Invivogen, CA, USA). The involvement of the TLR1/2 in signal transduction was tested using CU-CPT22 at 10 μM (Tocris Bioscience, UK). The used concentrations of inhibitors were selected based on recommendations provided by the manufacturers. The TLR4 knock-out RAW 264.7 cell line (RAW-Dual™ KO-TLR4, Inivogen, CA, USA) was used to evaluate the involvement of the TLR4 signaling pathway as these cells do not respond to TLR4 agonists. The inhibition studies were conducted using 10^6 RAW 264.7 cells or TLR4 knock-out RAW 264.7 cell line that were first seeded for 30 min in 24 well plates followed by 30 min pre-incubation with various inhibitors. Next, 10^6 heat- inactivated *P. agglomerans* bacterial cells were added to pre-treated RAW 264.7 cells in a final volume of 1 ml. The culture supernatants collected from non-stimulated cells and cells that were treated only with inhibitors were used as negative controls. The cultures were incubated for 24 hours, and afterwards supernatants were collected and used for cytokine quantification in ELISA.

Quantification of cytokines by ELISA and nitrite detection

The concentrations of TNF-α, IL-6, and IL-10 in culture supernatants were measured using ELISA Max Deluxe were from Biolegend® (CA, USA) according to manufacturer's instructions. Taking into account various detection limits of used ELISAs, culture supernatants were diluted 50 times for TNF-α, 100 times for IL-6, and 2 times for detection of IL-10 secretion. The detection limits for different cytokines were as follows (TNF-α/IL-6: 500 pg/ml, IL-10: 2.000 pg/ml). The nitrite concentrations were detected in culture supernatants using Griess reaction and a commercial kit from Promega (WI, USA) according to manufacturer's instructions. In this assay, undiluted culture supernatants were used after 24 hrs of stimulation of RAW 264.7 cells or TLR4 knock-out RAW 264.7 cells with *P. agglomerans* whole-cell preparation in the presence or absence of various inhibitors.

Statistical analysis

All values recorded in experiments were presented as mean ± standard error of the mean (SEM) of three independent experiments. Statistical analysis was conducted using a Student's t-test, with GraphPad Prism 5.0c software. Values with $P < 0.001$ were considered as significantly different.

Results

Genomic features of the *Pantoea agglomerans* KM1 isolate

Whole-genome sequencing of *P. agglomerans* KM1, using the Illumina HiSeq 4000 platform, resulted in approximately 168-fold genome coverage. Collectively, 6,890,002 raw reads of 101 bp in length were subjected to quality filtering with low quality scores (≤Q27) and a minimum length of 36 bases. After trimming, 6,323,946 (91.78%) clean reads were used for downstream analysis. *De novo* assembly of the sequence reads resulted in 46 contigs, and the N50 of the contigs was 330,495 bp. The maximum length of a contig was 1,299,234. BUSCO provides quantitative measures for the assessment of genome assembly based on evolutionarily informed expectations of gene content from near-universal single-copy orthologs. Evaluation of a genome completeness using BUSCO revealed that *P. agglomerans* KM1 was 99.2% complete, suggesting that most of the recovered genes could be classified as complete and single-copy. Moreover, the genome contained one fragmented BUSCO contributing to 0.8% of the total BUSCO groups (S1 Fig). Hence, as demonstrated in Fig 1, the draft genome sequence of

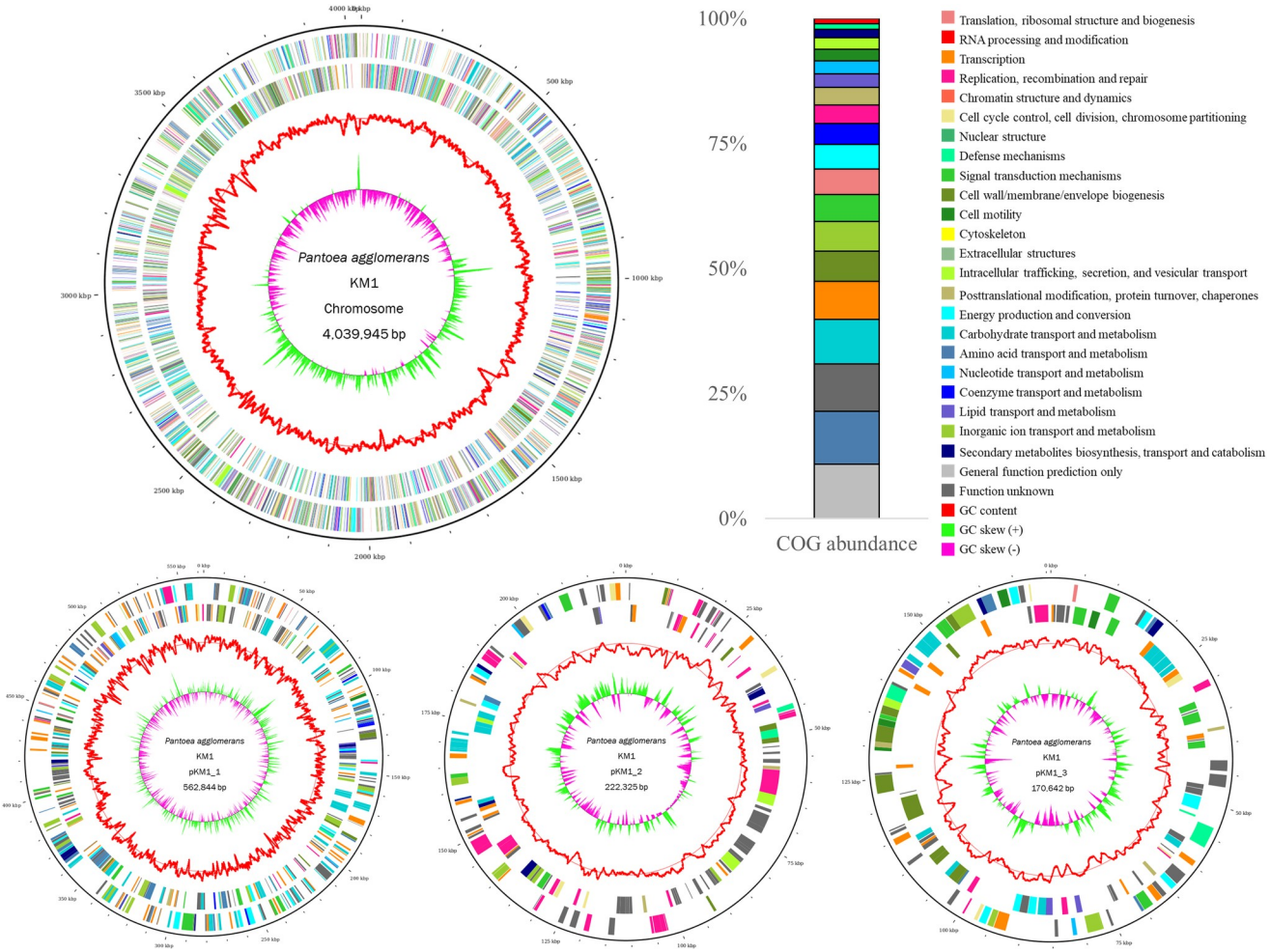

Fig 1. The circular genome maps of the *P. agglomerans* KM1 draft genome. Genome map showing the features of *P. agglomerans* KM1 chromosome and plasmids pKM1_1, pKM1_2, and pKM1_3. Circles illustrate the following from outermost to innermost rings: (1) forward CDS, (2) reverse CDS, (3) GC content, and (4) GC skew. All the annotated open reading frames (ORFs) are colored differently according to the COG assignments. Stacked bar chart shows the relative abundance (%) of COG categories calculated based on the total number of predicted ORFs present in the annotated genome.

https://doi.org/10.1371/journal.pone.0239792.g001

P. agglomerans KM1 included one circular DNA chromosome of 4,039,945 bp with a GC content of 55.55%. The KM1 chromosome contained 4,651 genes, of which 4488 were protein coding, 64 tRNAs, 1 rRNA and 9 ncRNAs. In addition to the bacterial chromosome, the genome consisted of three mega plasmids named pKM1_1, pKM1_2 and pKM1_3 of sizes 562,844 bp, 222,325 bp and 170,642bp, respectively. The number of protein-coding genes present on pKM1_1, pKM1_2, and pKM1_3 was 538, 237 and 152, respectively.

Genome annotation

The predicted Open Reading Frames (ORFs) were further classified into COG functional groups (Fig 1) and SEED Subsystem categories (S2 Fig). The top 5 most abundant COG category based on counts are class of R (702 ORFs, General function prediction only), class of E (270 ORFs, Amino acid transport and metabolism), class of C (258 ORFs, Energy production and conversion), class of J (245 ORFs, Translation, ribosomal structure and biogenesis) and class of L (238 ORFs, Replication, recombination and repair) categories. For SEED subsystem analysis, 36,697 ORFs were classified to SEED Subsystem categories (S2 Fig). Among the SEED categories, the top five most abundant categories were Carbohydrates (5865 ORFs), Amino Acids and Derivatives (5115 ORFs), Cofactors, Vitamins, Prosthetic Groups, Pigments (3026 ORFs), Protein Metabolism (2490 ORFs) and DNA metabolism (2242 ORFs) (S2 Fig). Fig 1 shows the circular genome maps of the KM1strain indicating all annotated ORFs and GC content using the GView program.

Phylogenetic analysis and comparative genomics

Phylogenetic tree analysis based on the concatenated sequences of six protein-coding housekeeping genes revealed that strain KM1 clustered closely with strains C410P1 and UAEU18 (Fig 2A). This analysis included closely related members in the genus *Pantoea* with publicly available genome sequences. The 16S rRNA gene sequences of the Enterobacteriaceae tend to provide insufficient resolution and the phylogenetic relationship of *P. agglomerans* was therefore inferred based on multilocus sequence analysis (MLSA). Whole genome phylogenetic tree based on OrthoANI values among *Pantoea* genome sequences revealed that strain KM1 had 79.12% to 98.66% genome sequence similarities with its closely related species (Fig 2B). The OrthoANI values between KM1 and other *Pantoea* genomes were as follows: *P. agglomerans* C410P1 (98.66%), *P. agglomerans* UAEU18 (98.68%), *P. agglomerans* IG1 (97.39%), *P. agglomerans* L15 (97.48%), *P. agglomerans* JM1 (97.41%), *P. agglomerans* TH81 (97.47%), *P. agglomerans* Tx10 (97.44%), *P. vagans* C9-1 (90.82%), and *P. ananatis* LMG 2655^{T} (79.12%). Our results showed that *P. agglomerans* KM1 clustered in the same clade with C410P1 (98.66%) and UAEU18 (98.68%), suggesting a common evolutionary origin.

Genome synteny analysis was performed to extend our understanding of the genomic characteristics of *P. agglomerans* KM1 (Fig 3). The genome alignment revealed the presence of 36 collinear blocks and several regions of translocations and inversions. In addition, the chromosomal alignments between strains C410P1 and KM1 are nearly identical, as shown by the presence of large collinear blocks of high similarity when most portions of the two chromosomes are aligned onto each other. Interestingly, the three plasmids of KM1 are syntenic with the three plasmids of C410P1 strain, where in plasmid pKM1_3 shows inversions relative to C410P1.

Genomic sequences involved in response to viruses and horizontal gene transfer

Twenty-two genomic islands (GIs) were identified on the chromosome of *P. agglomerans* KM1 (Fig 4 and S1 Table), suggesting horizontal DNA transfer. In the KM1 chromosome, GI region 4

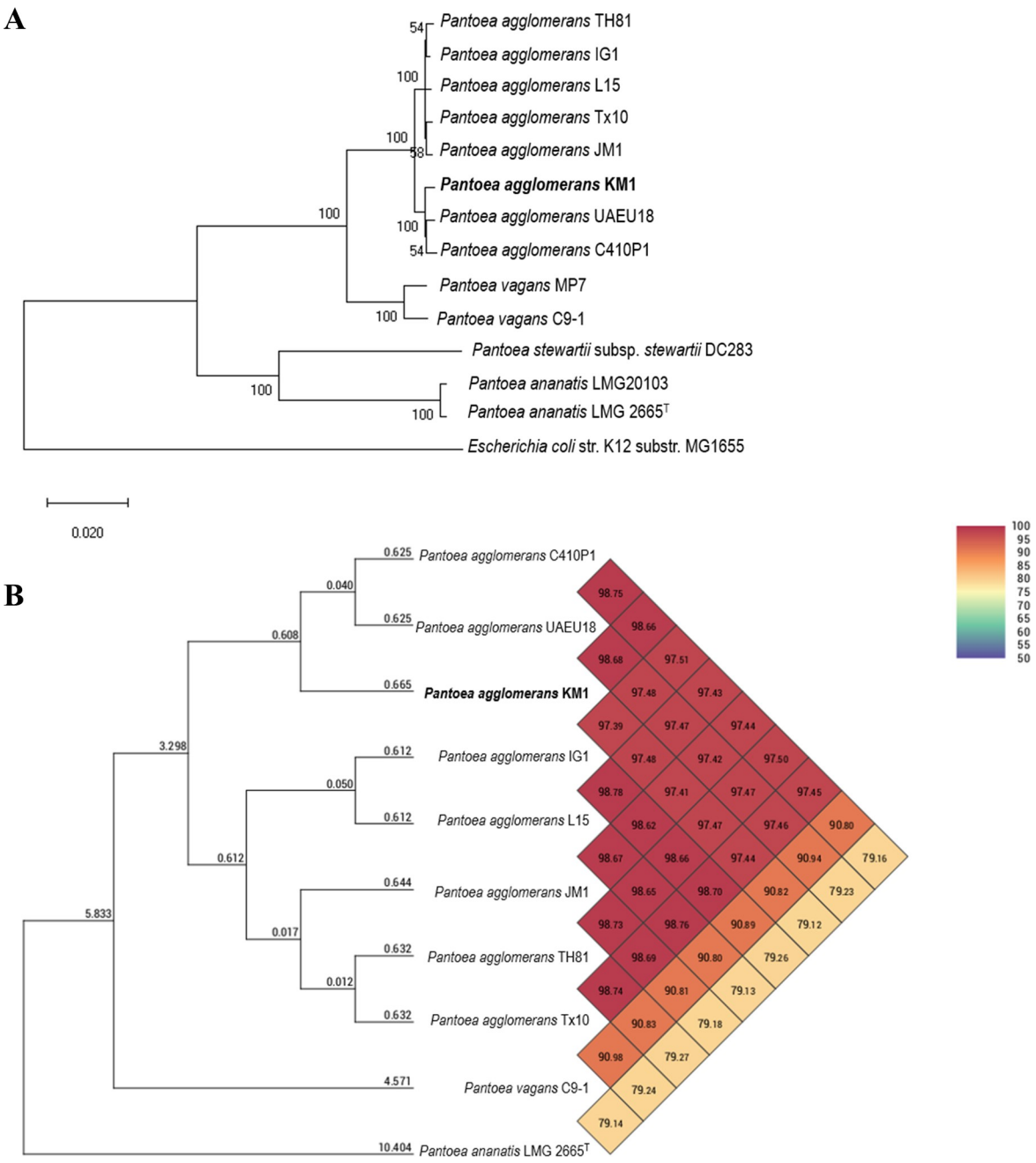

Fig 2. Phylogenetic analysis of *P. agglomerans* KM1. A: Neighbor-joining phylogenetic tree showing the phylogenetic relationship between *P. agglomerans* KM1 and selected *Pantoea* strains. The neighbor-joining tree was constructed from an alignment of concatenated *fusA*, *gyrB*, *leuS*, *pyrG*, *rplB*, and *rpoB* gene sequences. The percentage of replicate trees in which the associated taxa clustered together in the bootstrap test (1000 replicates) are shown next to the branches. Superscript "T" indicates a type strain. The scale bar represents the number of substitutions per site. *Escherichia coli* strain K12 substr. MG1655 was used as an outgroup. **B:** Heatmap showing the OrthoANI values between *P. agglomerans* KM1 genome and its closely related species. Values greater than 97% indicate that strains belong to the same species.

https://doi.org/10.1371/journal.pone.0239792.g002

was found to encode type I secretion proteins and GI region 16 encodes LysR-family transcriptional regulator, which are required for virulence. GI region 1 contained glutathione S-transferase, omega (EC 2.5.1.18), which serve as the primary defenses against oxidative stress [53] (S1

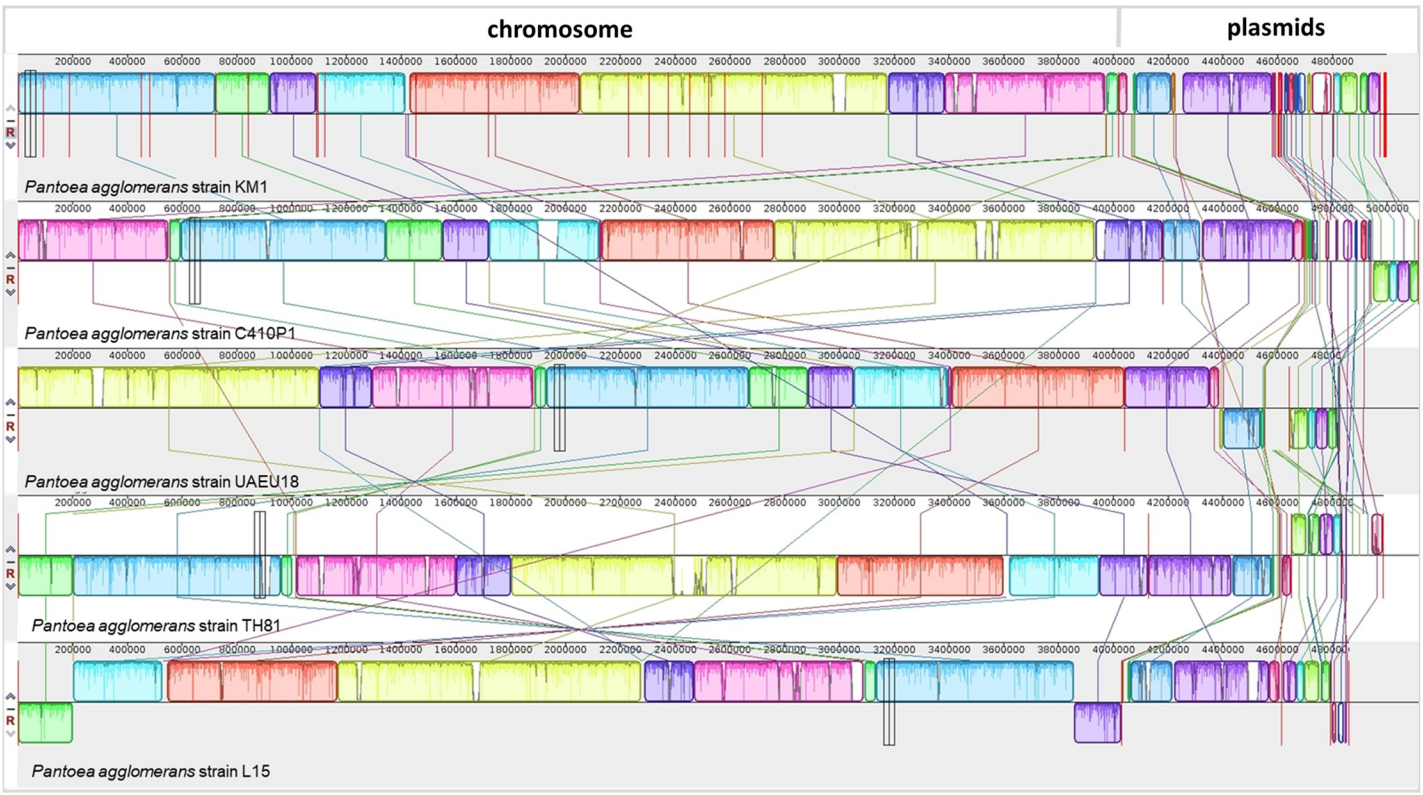

Fig 3. Genome alignments showing synteny blocks among *P. agglomerans* strains obtained using progressive Mauve. *P. agglomerans* KM1 were compared with other closely related strains namely C410P1, UAEU18, TH81 and L15. Each genome is laid out horizontally with homologous segment outlined as colored rectangles. Each same color block represents a locally collinear block (LCB) or homologous region shared among genomes. Rearrangement of genomic regions was observed between the two genomes in terms of collinearity. Inverted regions relative to KM1 are localized in the negative strand indicated by genomic position below the black horizontal centerline in the Mauve alignment.

https://doi.org/10.1371/journal.pone.0239792.g003

Table). Additionally, 4, 2, and 2 GIs were detected on KM1 plasmids pKM1_1, pKM1_2, and pKM1_3, respectively (Fig 4). Plasmid pKM1_1 harbored genes involved in carotenoid biosynthesis including lycopene cyclase (*CrtY*), zeaxanthin glucosyltransferase (*CrtX*) and geranylgeranyl diphosphate synthase (*CrtE*), suggesting that *P. agglomerans* KM1 is a carotenogenic bacterium, where carotenoids serve an essential role in protection against oxidative stress and protection from oxygen during nitrogen fixation [54] (S1 Table). Using PHASTER, two prophage regions were predicted in KM1 chromosome, where GI regions 6 to 13 coincide with prophage region 1, and GI region 20 to 21 incorporates prophage region 2 (Fig 4 and S4 Fig). Prophage region 1 is an intact prophage with a size of 52 kb, a GC content of 52.56%, and 82 ORFs in the phage protein database. Prophage region 2 is an incomplete prophage and it has a size of 12.9 kb, with a GC content of 47.26%, and 13 ORFs. Several genes that have a phage-derived genetic material were present in the KM1 chromosome such as a phage integrase, a phage lysozyme, a phage terminase, a phage tail tip, a phage capsid and a scaffold protein. The *P. agglomerans* KM1 genome also contained six CRISPR loci (CRISPR1-CRISPR6) with direct repeats ranging between 23 to 42 and mean size spacers ranging from 35 to 59 (S2 Table).

Biochemical characterization

Biochemical analysis of the *P. agglomerans* KM1 was conducted using an API 20E test (S3 Table). The isolate was catalase positive and scored negative in the oxidase and urease

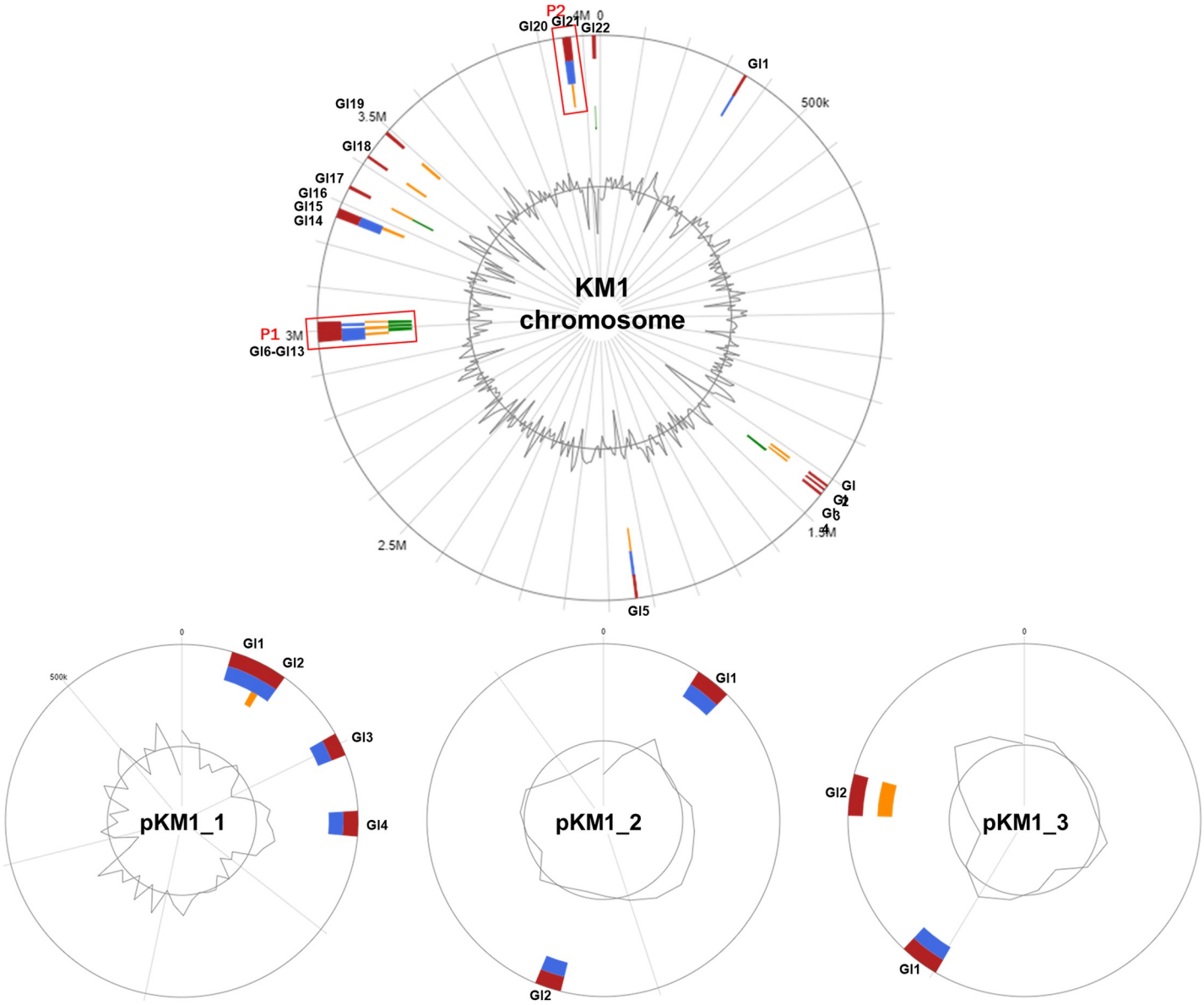

Fig 4. Genomic islands (GIs) in *P. agglomerans* strain KM1 predicted using IslandViewer4. The predicted genomic islands are colored based on the prediction methods. Red indicates an integrated analysis, blue represents IslandPath-DIMOB prediction, orange represents SIGI-HMM prediction, and green indicates IslandPick analysis. The circular plots show the genomic islands in *P. agglomerans* KM1 chromosome, and plasmids pKM1_1, pKM1_2 and pKM1_3. GIs are labelled in blue. Prophage regions predicted by PHASTER were indicated in red boxes for prophage region 1 (P1) and region 2 (P2).

https://doi.org/10.1371/journal.pone.0239792.g004

test. KM1 did not decarboxylate lysine and ornithine, nor produced hydrogen sulfide (H_2S) and indole. In addition, the isolate was able to ferment D-glucose, D-mannitol, L-rhamnose, D-sucrose, Amygdalin, L-arabinose and Lactose. The API 20E test was negative for arginine dihydrolase and tryptophan deaminase. The KM1 isolate had no ability to ferment inositol, D-sorbitol, and D-melibiose, however, it showed positivity in acetoin production, β-galactosidase test, citrate utilization test, and possessed gelatinase activity. Obtained numerical profile confirmed that isolated KM1 strain belongs to *P. agglomerans* species.

Genes involved in antibiotic resistance

The presence of Antibiotic Resistance Genes (ARGs) was identified using BLAST against the CARD reference sequences (S4 Table). We identified 12 ARGs in KM1 chromosome and 1 ARG in plasmid pKM1_3 showing greater than 70% identity to well-characterized ARGs in CARD database. The ARGs identified in KM1 were classified into five gene families including resistance-nodulation-cell division (RND) antibiotic efflux pump (*CRP*, *oqxB*, *mdtA*, *mdtB*, *mdtC*, *acrR*, *acrD*, and *MuxB*), ATP-binding cassette (ABC) antibiotic efflux pump (*msbA*), major facilitator superfamily (MFS) antibiotic efflux pump (*emrA* and *emrB*), undecaprenyl-pyrophosphate related protein (*bacA*) and family of phosphoethanolamanine transferase (*arnA*). These genes provide resistance to multiple antibiotic classes such as macrolides, fluoroquinolones, tetracyclines, aminoglycosides, nitroimidazoles aminocoumarins, and peptide based antibiotics. The predicted multidrug resistant genes present in KM1 genome were primarily involved into two resistance mechanisms namely antibiotic efflux and antibiotic target alteration. These results are consistent with data obtained from the Kirby-Bauer disk diffusion test showing that KM1 strain is resistant to penicillin G, vancomycin, bacitracin, fosfomycin, and rifampicin (Table 1).

Genes involved in adaptations to environmental stress

In the past, *P. agglomerans* strains have been isolated from a multitude of environments such as extreme desiccation in powdered infant milk formula [10], broad range of temperature (3–42 ^{o}C) or pH (5–8.6) regimes [55] and osmotically challenging environments [56], as such its survival in stressful environments have not been examined so far at the molecular level. Table 2 demonstrates the list of genes found in the KM1 isolate, associated with resistance to stressful environmental conditions. Several genes encode products involved in osmoregulation included aquaporin Z (*aqpZ*), osmotically inducible protein (*OsmY*), potassium transporter protein (*TrkH* and *TrkA*), glycine betaine transporter protein (*proP*), trehalose-6-phosphate synthase (*otsA* and *otsB*), and glutathione-regulated potassium-eflux system protein (*kefB*). Further in-depth analysis revealed the presence of genes coding for proteins involved in adaptation to temperature fluctuations such as cold shock proteins (*cspA*, *cspE*, and *cspD*) and heat shock proteins (*DnaJ*, *DnaK*, *GrPE*, *hslR*, *IbpA*, *hspQ*). Finally, genes conferring resistance to oxidative stress were also detected in KM1 strain such as catalase (*katE*, *katG*), superoxide dismutase (*sodA*), glutathione S-transferase (*GST*), glutathione peroxidase (*GPX*), and DNA protection during starvation protein (*Dps*).

Table 1. Antibiotic susceptibility profile of *P. agglomerans* KM1.

Antibiotic	Amount	Inhibition zone diameter (mm)[a]	Resistant/Susceptible
Imipenem	10 μg	32	Susceptible
Ampicillin	30 μg	21	Susceptible
Penicillin G	10 U	13	Resistant
Vancomycin	10 μg	0	Resistant
Bacitracin	10 μg	0	Resistant
Fosfomycin	50 μg	0	Resistant
Kanamycin	30 μg	20	Susceptible
Streptomycin	10 μg	17	Susceptible
Chloramphenicol	30 μg	30	Susceptible
Rifampicin	5 μg	12	Resistant
Ofloxacin	5 μg	39	Susceptible

[a] Values are expressed as means from three independent experiments.

https://doi.org/10.1371/journal.pone.0239792.t001

Table 2. Genes associated with resistance to environmental stress in *P. agglomerans* KM1.

Environmental stress resistance	Annotation	Locus tag
Osmotic stress		
OsmY	Osmotically-inducible protein Y	HBB05_RS01050
aqpZ	Aquaporin Z	HBB05_RS05300
TrkH, *TrkA*	Trk system potassium transporter protein	HBB05_RS05080, HBB05_RS02110
proP	Glycine betaine/L-proline transporter	HBB05_RS19460, HBB05_RS02985
proQ	RNA chaperone ProQ	HBB05_RS14815
otsA, *otsB*	Trehalose-6-phosphate synthase	HBB05_RS15190, HBB05_RS15195
kefB,	Glutathione-regulated potassium-efflux system protein	HBB05_RS02355, HBB05_RS02360
TreF	Cytoplasmic trehalase	HBB05_RS00975
Heat shock		
DnaJ, *DnaK*	Molecular chaperone DnaJ	HBB05_RS18860, HBB05_RS19155, HBB05_RS07025, HBB05_RS07020
hslR	Ribosome-associated heat shock protein Hsp15	HBB05_RS02565
IbpA, *hspQ*	Heat shock protein	HBB05_RS04290, HBB05_RS10600
GrpE	Nucleotide exchange factor	HBB05_RS18265
Cold shock		
cspA, *cspE*, *cspD*	Cold shock protein	HBB05_RS19980, HBB05_RS03250, HBB05_RS09100, HBB05_RS10245
Oxidative stress		
dps	DNA protection during starvation protein	HBB05_RS09995, HBB05_RS00870
oxyR,	DNA-binding transcriptional regulator	HBB05_RS03440
Gpx	Glutathione peroxidase	HBB05_RS19175, HBB05_RS03445, HBB05_RS12185
Gst	Glutathione S-transferase	HBB05_RS18795, HBB05_RS18945, HBB05_RS19010, HBB05_RS20560, HBB05_RS01550, HBB05_RS03195, HBB05_RS03320, HBB05_RS04480, HBB05_RS05500
KatE, *katG*	Catalase	HBB05_RS12490, HBB05_RS16130
sodA	Superoxide dismutase	HBB05_RS04520, HBB05_RS12380

https://doi.org/10.1371/journal.pone.0239792.t002

Genome-based identification of virulence factors

The putative virulence factors in *P. agglomerans* KM1 were predicted by BLAST searches against the VFDB and genome annotation using NCBI PGAP. As demonstrated in Table 3, identified virulence factors were classified into five categories including secretion systems, adhesion, motility, iron uptake/sequestration system and toxins.

In the secretion system category, all the putative genes belonging to type VI secretion system (T6SS) were present. The genes encoding the complete structural gene components of the T6SS apparatus consisted of *TssA-TssM*, hemolysin-coregulated protein (*Hcp*), valine-glycine repeat G (*VgrG*) protein, proline-alanine-alanine-arginine repeats (*PAAR*) and *ClpV*. In addition, the presence of T6SS hallmarks *Hcp* and *VgrG* genes in KM1 was validated using PCR and amplicon sequencing (S5 Fig). The latter showed 100% sequence identity to *Hcp* and *VgrG* proteins in *P. agglomerans*. In the adhesion category, the identified genes encoded filamentous hemagglutinin (*FHA*) and the outer membrane protein A (*OmpA*). In the motility category, genes involved in flagella were detected in KM1, which play roles in biofilm formation, virulence factor secretion and adhesion in addition to motility [57]. In the iron uptake category, chromosomal genes encoding proteins related to iron uptake and transport included ferric

Table 3. Virulence factors of *P. agglomerans* KM1.

Virulence factor	Annotation	Locus tag
Secretion system		
TssA, *TssB*, *TssC*, *TssD* (*Hcp*), *TssE*, *TssF*, *TssG*, *TssH* (*ClpV*), *TssI* (*vgrG*), *TssJ*, *TssK*, *TssL* (*DotU*), *TssM* (*IcmF*), *tagF*, *tagH*, *PAAR*	Type VI secretion protein	HBB05_RS11570, HBB05_RS11575, HBB05_RS11580, HBB05_RS11585, HBB05_RS11590, HBB05_RS11595, HBB05_RS11600, HBB05_RS11605, HBB05_RS11615, HBB05_RS11650, HBB05_RS11670, HBB05_RS11675, HBB05_RS11680, HBB05_RS11685, HBB05_RS11700, HBB05_RS11705, HBB05_RS11710, HBB05_RS11900, HBB05_RS11905, HBB05_RS11910, HBB05_RS17335, HBB05_RS17360, HBB05_RS17365, HBB05_RS17370, HBB05_RS17375, HBB05_RS17380, HBB05_RS17385, HBB05_RS17410, HBB05_RS17415, HBB05_RS17420, HBB05_RS17435, HBB05_RS17440, HBB05_RS17445, HBB05_RS18610, HBB05_RS18655, HBB05_RS17395
Adhesion		
fha	Filamentous hemagglutinin	HBB05_RS03515, HBB05_RS04420, HBB05_RS11225, HBB05_RS15615
ompA	Outer membrane protein A	HBB05_RS19865, HBB05_RS04215, HBB05_RS10555, HBB05_RS11915, HBB05_RS17425
Motility		
fliC, *fliD*, *fliE*, *fliF*, *fliG*, *fliH*, *fliI*, *fliJ*, *fliK*, *fliL*, *fliM*, *fliN*, *fliO*, *fliQ*, *fliS*, *fliT*,*fliZ*, *flhA*, *flhC*, *flhD*, *flhE*, *flgA*, *flgB*, *flgC*, *flgD*, *flgE*, *flgF*, *flgG*, *flgH*, *flgI*, *flgJ*, *flgK*, *flgL*, *flgN*, *motB*	Flagella	HBB05_RS15305, HBB05_RS15310, HBB05_RS15315, HBB05_RS15320, HBB05_RS15410, HBB05_RS15415, HBB05_RS15420, HBB05_RS15425, HBB05_RS15430, HBB05_RS15435, HBB05_RS15440, HBB05_RS15445, HBB05_RS15450, HBB05_RS15455, HBB05_RS15460, HBB05_RS15470, HBB05_RS15285, HBB05_RS15115, HBB05_RS15180, HBB05_RS15185, HBB05_RS15110, HBB05_RS11030, HBB05_RS11035, HBB05_RS11040, HBB05_RS11045, HBB05_RS11050, HBB05_RS11055, HBB05_RS11060, HBB05_RS11065, HBB05_RS11070, HBB05_RS11075, HBB05_RS11080, HBB05_RS11085, HBB05_RS11020, HBB05_RS15170
CheV, *CheY*, *CheW*, *CheA*	Chemotaxis protein	HBB05_RS21255, HBB05_RS08110, HBB05_RS12020, HBB05_RS15130, HBB05_RS15160, HBB05_RS15165, HBB05_RS15645
Iron uptake system		
fur	Ferric iron uptake transcriptional regulator	HBB05_RS09340
EfeO	Iron uptake system protein	HBB05_RS15240
SitC	Iron/manganese ABC transporter permease subunit	HBB05_RS21090
fepB,*fepG*, *entS*	Enterobactin transporter	HBB05_RS06140, HBB05_RS06155, HBB05_RS06145
fepA	TonB-dependent siderophore receptor	HBB05_RS20475, HBB05_RS21020, HBB05_RS06180
fepD	Ferric siderophore ABC transporter permease	HBB05_RS06150
fhuF	Siderophore-iron reductase	HBB05_RS06780
Toxin		
Hha, *ShlB*, *FhaC*, *HecB*, *XhlA*	Hemolysin	HBB05_RS23025, HBB05_RS03510, HBB05_RS04405, HBB05_RS08630, HBB05_RS11220, HBB05_RS14060, HBB05_RS15620
hlyIII	Hemolysin III	HBB05_RS00635

https://doi.org/10.1371/journal.pone.0239792.t003

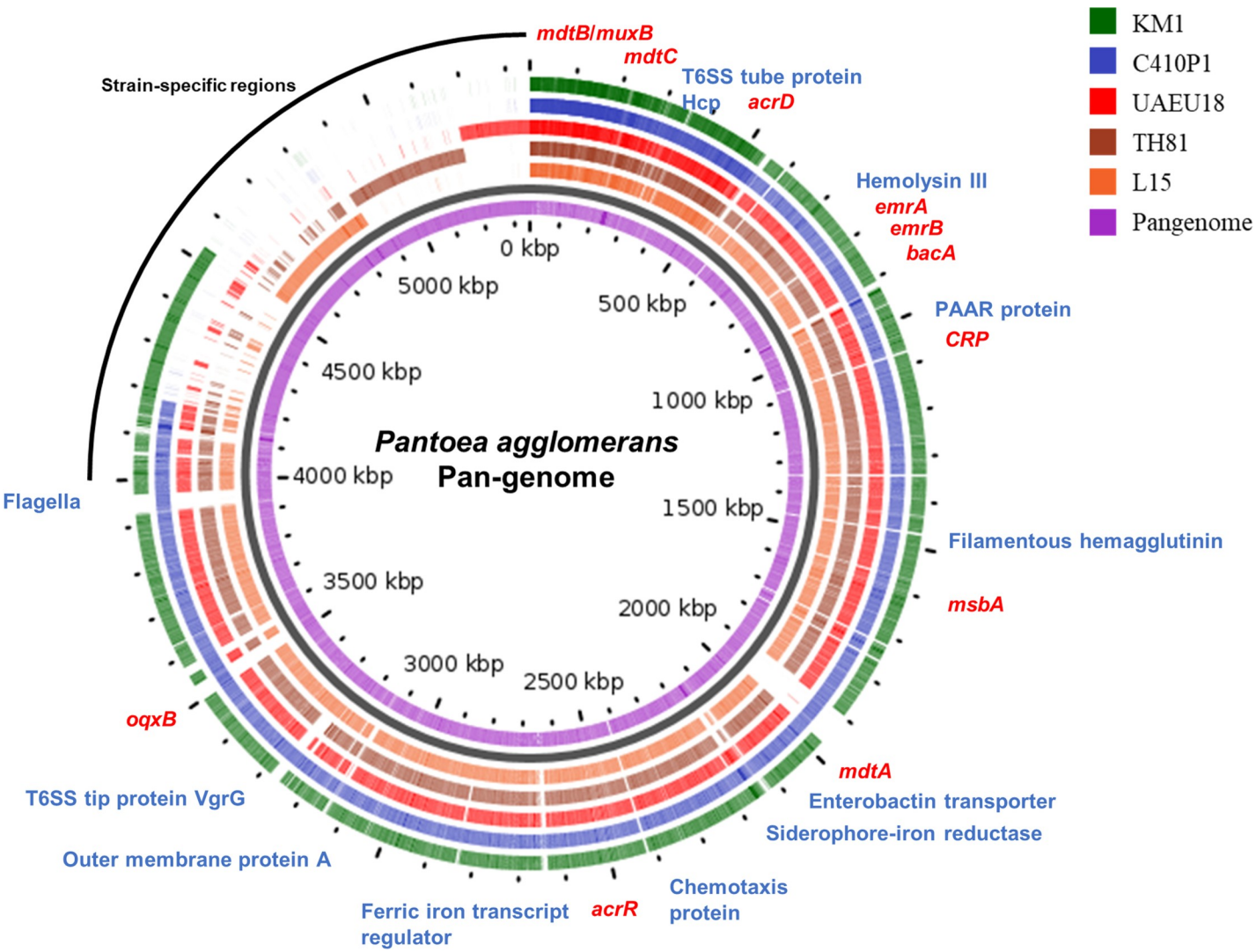

Fig 5. Pan-genome analysis of *P. agglomerans* strains obtained using Gview server. The innermost circle shows the pan-genome (purple), and outer circlers indicate the genomes of *Pantoea agglomerans* strains L15 (orange), TH81 (brown), UAEU18 (red), C410P1 (blue), and KM1 (green). Genes with specialized functions were labelled with different colors: virulence-related genes (blue), antibiotic resistance genes (red), and strain-specific regions (black).

https://doi.org/10.1371/journal.pone.0239792.g005

iron uptake transcriptional regulator (*fur*), iron uptake protein (*EfeO*). Plasmid pKM1_3 contained the iron/manganese ABC transporter permease (*SitC*). In addition, genes related to high-affinity iron-chelating molecules i.e. siderophores, encompassed the enterobactin transporter (*fepB*, *fepG*, *entS*), TonB-dependent siderophore receptor (*fepA*), ferric siderophore ABC transporter permease (*fepD*, and siderophore-iron reductase (*fhuF*). The last group of virulence factors contained genes coding for extracellular cytotoxic proteins hemolysin III, hemolysin *XhlA*, and hemolysin secretion/activation genes (*Hha*, *ShlB*, *FhaC*, *HecB*).

A pan-genome map for the KM1 strain and four other completely sequenced *P. agglomerans* strains L15, TH81, UAEU18 and C410P1 was drawn using PGAP and Gview server (Fig 5). Pan-genome analysis revealed that the T6SS effector proteins *Hcp* and *VgrG* were detected in all five strains. Moreover, the hemolysin transporter protein *ShlB*, adhesion protein (*ompA*), iron uptake genes (*fur*, *EfeO*, *fepA*, *fepD*, *fhuF*, *fepB*, *fepG*, *entS*), chemotaxis proteins (*CheV*, *CheY*, *CheW*, *CheA*) and flagellin (*fliC*) were present in all strains. Interestingly, RND

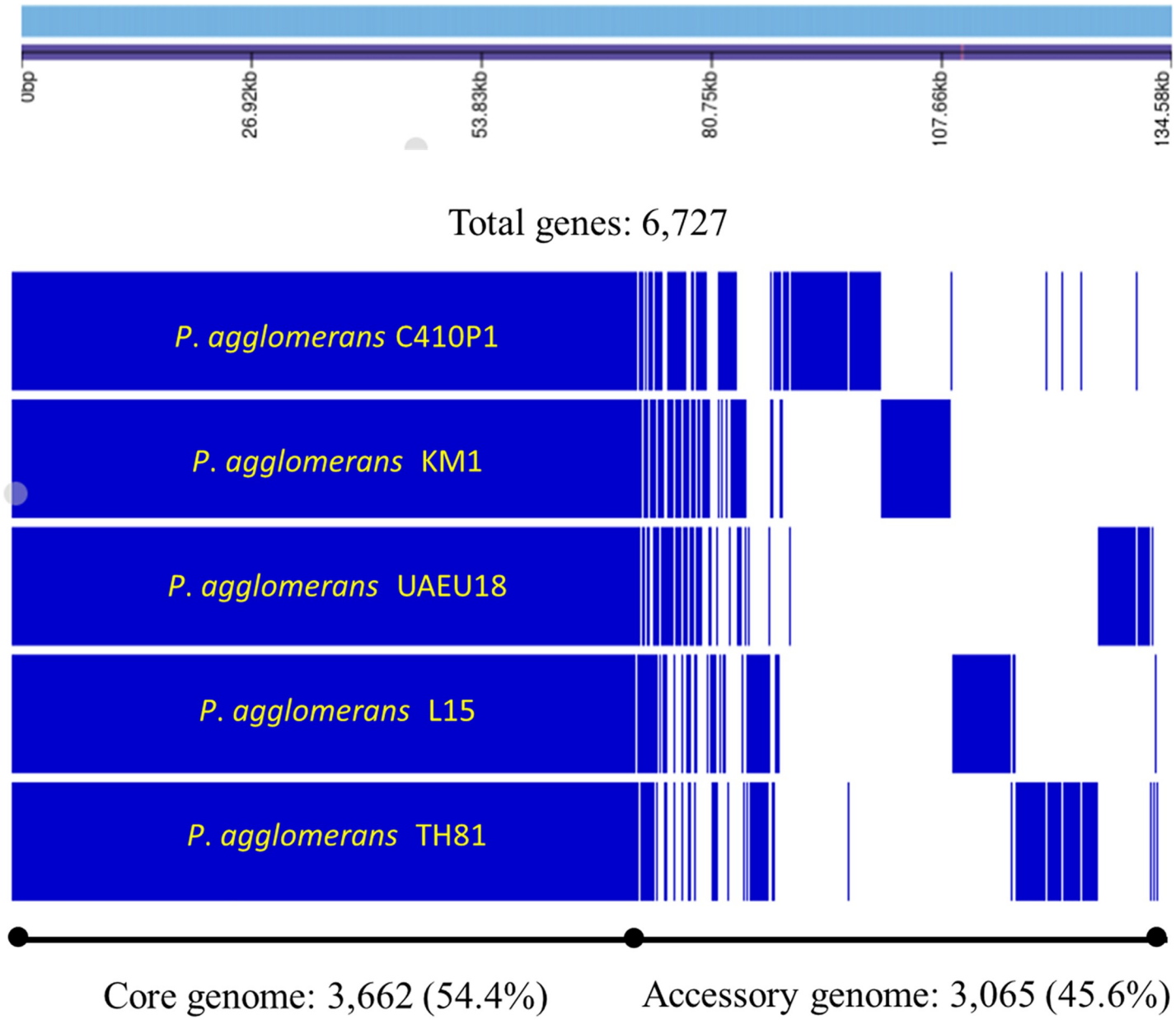

Fig 6. Roary matrix-based pan-genome analysis of *P. agglomerans* strains. The core-genome tree generated was compared with a matrix where the core and accessory genes were either present (blue) or absent (white).

https://doi.org/10.1371/journal.pone.0239792.g006

antibiotic efflux pump associated genes (*CRP*, *oqxB*, *mdtA*, *mdtB*, *mdtC*, and *acrR*) were detected in all five strains. These findings indicated that virulence factors and ARGs identified in this study might play important roles in the potential pathogenicity of *P. agglomerans*.

Based on Roary-matrix pipeline, the pan-genome analysis of five *P. agglomerans* strains revealed 6,727 protein coding genes comprising the pan-genome, of which 3,065 genes (45.6%) corresponded to the accessory genome and 3,662 genes (54.4%) to the core genome (Fig 6). As the *P. agglomerans* pan-genome increases with the addition of new strains, the size of core genome decreases, suggesting that *P. agglomerans* has an open pan-genome [58] (S3 Fig).

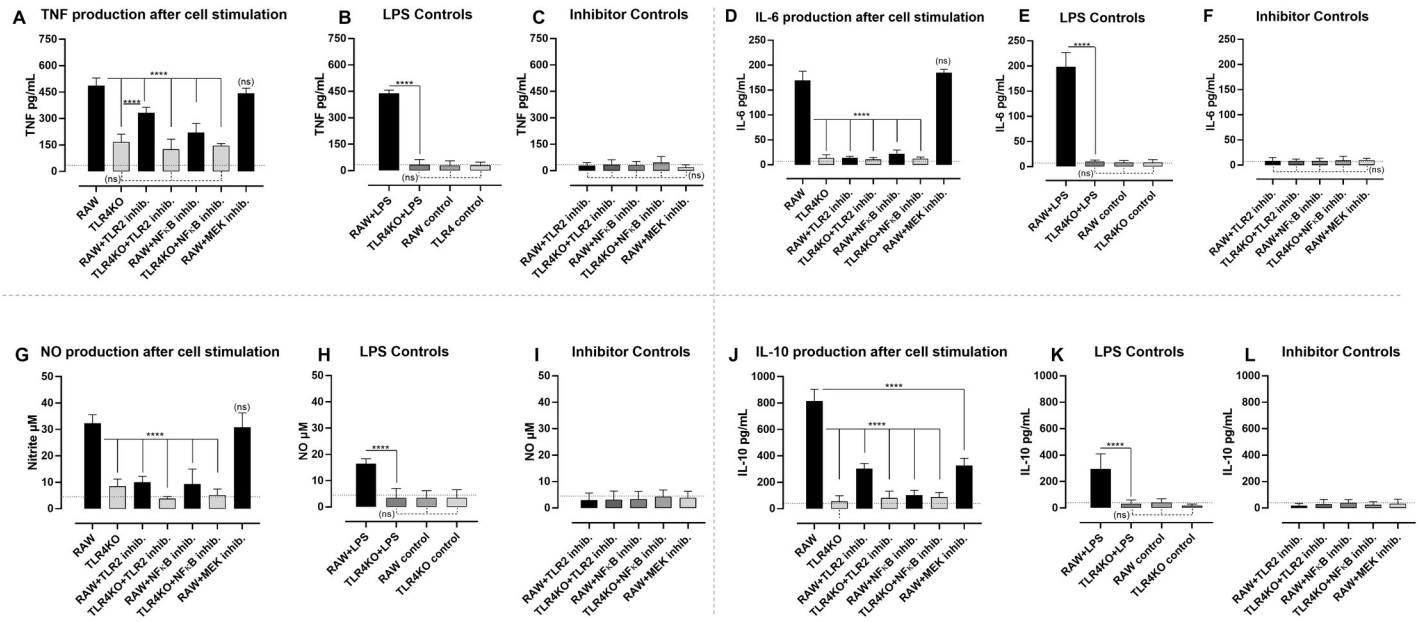

Fig 7. Cytokine and nitrite production by RAW 264.7 macrophages stimulated with a heat inactivated whole-cell *P. agglomerans*. Panels A, D, G and J show TNF-α, IL-6, Nitrite and IL-10 secretion by the simulated RAW 264.7 cells (RAW), TLR4 knock-out RAW 264.7 cells (TLR4KO), RAW 264.7 cells (RAW) in combination with TLR2 inhibitor (RAW+ TLR2 inhib), TLR4 knock-out RAW 264.7 cells in combination with TLR2 inhibitor (TLR4KO + TLR2 inhib.). Additionally stimulations were performed using RAW 264.7 cells in combination with NFκB inhibitor (RAW+NFκB inhib.), TLR4 knock-out RAW 264.7 cells in combination with NFκB inhibitor (TLR4KO + NFκB inhib.) and RAW 264.7 cells in combination with MEK1/2 inhibitor (RAW + MEK inhib.). Panels B, E, H, and K, include control conditions: RAW 264.7 cells stimulated with TLR4 agonist ultrapure LPS (RAW + LPS), TLR4 knock-out RAW 264.7 cells stimulated with TLR4 agonist ultrapure LPS (TLR4KO + LPS), non-stimulated RAW 264.7 cells (RAW control), non-stimulated TLR4 knock-out RAW 264.7 cells (TLR4 control). Panels C, F, I and L include control stimulations: RAW 264.7 cells and TLR4 knock-out RAW 264.7 cells in the presence of inhibitors alone, RAW + TLR2 inhibitor, TLR4KO + TLR2 inhibitor, RAW + NFκB inhibitor, TLR4KO + NFκB inhibitor, and RAW + MEK inhibitor. Values with $P < 0.001$ were considered as significantly different (****).

https://doi.org/10.1371/journal.pone.0239792.g007

Immuno-stimulatory potential of *P. agglomerans KM1*

In order to supplement the genomic virulence study with additional data on the potential contribution of *P. agglomerans* KM1 to induction of inflammation, the immuno-stimulatory properties of the KM1 isolate were tested *in vitro* using the RAW 264.7 macrophage cell line. The latter was stimulated with a heat-inactivated whole-cell preparation of the KM1 isolate, followed by the measurement of cytokine secretion and Nitric Oxide (NO) production. The mechanisms underlying KM1-associated production of cytokines and NO were tested by inhibiting TLR1/2 and TLR4 signaling and activation of NF-kB and MAPK Kinases, such as MEK 1 and MEK2.

As shown in Fig 7A, stimulations of RAW 264.7 macrophages with *P. agglomerans* KM1 resulted in the production of TNF-α. Under identical stimulation conditions RAW 264.7 TLR4 knock-out cells exhibited a significantly reduced TNF-α secretion. Analysis of a possible involvement of the TLR1/2 signaling in TNF-α secretion by stimulated RAW 264.7 macrophages showed partial reduction in the presence of the CU-CPT22 TLR-1/2 inhibitor. However, this inhibitory effect was itself significantly less potent than the effect observed in the TLR4 knock-out condition. Adding CU-CPT22 to stimulated TLR4 knock-out cells did not result in an additional inhibitory effect, indicating a dominant role of the TLR4 signaling. The use of inhibitors of intracellular pathways leading to activation of the NF-κB (Bay 11–7082) and MAPKKs (UO126) allowed to further analyze mechanisms underlying KM1 associated TNF-α secretion. The use of Bay 11–7082 resulted in a significant reduction of TNF-α secretion by RAW 264.7 cells, similar to the inhibition observed in the absence of the TLR4

receptor. There was no added effect of the inhibitor in the TLR4 knock-out stimulation setting. Finally, we did not observe any inhibitory effect of the UO126, indicating a lack of the involvement of MAPK Kinases in *P. agglomerans* induced TNF-α secretion. In order to assess the results, the experimental setting was accompanied by a series of control conditions. First, RAW 264.7 cells and the RAW 264.7 TLR-4 knock-out cell line were both stimulated with ultra-pure LPS, showing the effectiveness of the absence of TLR4 in the inhibition of TNF-α secretion (Fig 7B). Under non-stimulated conditions, neither of the cell lines produced any measurable level of TNF-α. Finally, none of the inhibitors used in this study was able to drive TNF-α secretion by itself (Fig 7C)

To evaluate the capacity *P. agglomerans* to trigger IL-6 production by RAW 264.7 cells, an identical experimental set-up was used as the one described above. Here, the results presented in Fig 7D show that high levels of cytokine production were obtained by *P. agglomerans* stimulation of RAW 264.7 cells, but not RAW 264.7 TLR4 knock-out cells. In contrast to the partial inhibition of TNF- α production by CU-CPT22, addition of this TLR1/2 inhibitor resulted in a complete abolishment of IL-6 production. The same level of inhibition was also obtained by blocking the NF-κB signaling pathway alone or in combination with inhibition of TLR function. Blocking of MAPK Kinases did not result in reduction of IL-6 production. As for the TNF-α induction experiment, all necessary control culture conditions were included, showing the potency of the TLR4 knock-out construct in the inhibition of LPS-induced cytokine production (Fig 7E), as well as the lack of significant IL-6 induction by any of the inhibitors alone, used in this study (Fig 7F).

Next, the secretion of NO, an important pro-inflammatory effector molecule was analyzed using the same experimental setting. The presence of NO in culture supernatant can be measured using Griess reaction recording levels of a nitrite. As showed in Fig 6G, while *P. agglomerans* stimulated RAW 264.7 cells produced NO, interrupting either TLR4 or TLR1/2 signaling, resulted in a significant reduction of NO production. Inhibition of NO production was obtained by blocking of the NF-κB signaling, but not the MAPK Kinase pathway. As for the experiments outlined above, all cell culture control conditions were included, allowing proper result interpretation (Fig 7H and 7I.)

Finally, the potential of *P. agglomerans* to induce the anti-inflammatory cytokine IL-10 was analyzed. Results in Fig 7J show that stimulated RAW 264.7 cells produced IL-10 in a TLR1/2/4 and NF-κB dependent manner. As opposed to TNF-α, IL-6 and NO induction, the MAPK Kinases pathway appeared to contribute to triggering of IL-10 secretion, as the MEK 1 and MEK 2 inhibitors had a significant effect. All control conditions showed the validity of the *in vitro* experimental setup (Fig 7K and 7L).

Discussion

This study provides the comprehensive genomic and immunologic analysis of the foodborne *P. agglomerans* KM1 strain, that was isolated from homemade kimchi, a traditional South Korean fermented side dish prepared using Baechu cabbage (*Brassica rapa* subsp. *pekinensis*) as the main ingredient. Hence the origin of the KM1 stain is most probably the Baechu cabbage itself, as *P. agglomerans* was shown to grow as an epiphyte on vegetables and fruits [59, 60]. The analysis of the KM1 genomic data led to the identification of several virulence genes such as the genes associated to the type VI secretion system (T6SS), adhesion, iron uptake and sequestration system, as well as secretion of toxins such as hemolysins.

In the secretion system category, the KM1 strain harbors the complete structural gene components of the T6SS. Human pathogenic *Pseudomonas aeruginosa* and *Vibrio cholera* were shown to possess T6SS, which functions as a delivery apparatus of bacterial toxins into the host

cells [61, 62]. The *Hcp* is regarded as one of the secreted effectors of T6SS and it forms a tube in the outer component of the T6SS apparatus [61]. Moreover, we also detected the gene encoding the *VgrG* spike protein and PAAR domain-containing protein, which facilitates the translocation of effector proteins to mediate microbe-host interactions [63, 64]. In addition, the ATPase *ClpV* disassembles the contracted tail sheath, which enables a new T6SS complex to be reassembled from the released subunits [65]. In *Pantoea ananatis*, the T6SS complex plays important roles related to its pathogenicity, host range determination, niche adaptation and competition through killing of neighboring bacteria [66]. In *Francisella tularensisis* subsp. *tularensis*, the causative agent of the life-threatening zoonotic disease tularemia, T6SS is essential for entry and multiplication within host macrophages [67]. As such, the T6SS is a versatile protein secretion machinery that is able to target eukaryotic cells, highlighting its importance in the context of infection and disease [65]. In case of the isolated KM1 strain, the presence of T6SS may increase its fitness in relation to the host-associated microbial communities or cause pathology to neighboring host cells during infection.

In the adhesion category, FHA is an important virulence factor that is required for adhesion to the epithelial cells of mammalian hosts [68]. *Bordetella pertussis* uses FHA as a major adhesion protein to attach itself to the host cells and at the same time increasing the adherence of other pathogens [69]. *OmpA* has essential roles in bacterial adhesion, invasion, and intracellular survival along with evasion of host defenses or stimulators of pro-inflammatory cytokine production [70]. Thus, these findings indicate that *FHA* and *OmpA* in KM1 may have potential pathogenic roles in life-threatening lower respiratory tract infections and urinary tract infections associated to *P. agglomerans* [12].

The KM1 strain also harbors genes involved in hemolysis. These genes code for extracellular cytotoxic proteins, which are known virulence factors that target cell membranes causing erythrocyte lysis [71]. The last category of identified virulence factors includes genes associated with an iron uptake and siderophore mediated iron sequestration. Iron is an important element for survival and colonization by bacteria since it plays a crucial role in the electron transport chain to produce energy [72]. Iron acquisition systems are used by bacteria to scavenge iron from the environment under iron-restricted conditions [73]. Therefore, successful competition for iron is crucial for pathogenicity. Ferric uptake regulator (*Fur*) is a transcription factor that upregulates virulence factors in bacteria during iron depletion [74]. These findings suggest the ability of KM1 to survive in the blood and its potential ability to invade the central nervous system by crossing the blood-brain barrier as have been observed in *Cronobacter sakazakii* [75]. Interestingly, the presence of ferric siderophore enterobactin transporter in KM1 may facilitate extraction of iron from host-iron complexes like lactoferrin, transferrin, and hemoglobin [73]. Taken together, these results suggest that siderophore system could be an essential genetic determinant for growth, virulence and potential pathogenicity of *P. agglomerans* KM1.

The genomic data and results obtained from the Kirby-Bauer disk diffusion method pointed out that KM1 genome carried 13 antibiotic resistance genes conferring resistance to clinically important antibiotics among them penicillin G, bacitracin, vancomycin, rifampicin and fosfomycin. However, genome-based analysis was not able to predict the specific ARGs that confer resistance to the antibiotics that KM1 was resistant to except for *bacA*, which confers resistance to bacitracin. Recently, Su et al. suggested that these limitations of genome-based prediction arise from scarcity of genetic basis of resistance for some antibiotics [76]. These findings suggest that there is a need for better standardization of ARG annotation to facilitate accurate detection of ARGs Previously published clinical reports demonstrated that *P. agglomerans* can be responsible for a wide range of infections encompassing pneumonia, bladder and wound/skin infections, septicemia and meningitis [77]. While bacitracin is an

antibiotic prescribed against skin infections, fosfomycin is an effective drug against bladder infections [78–80]. Vancomycin is used to treat meningitis, and rifampicin exerts antimicrobial activity against *Mycobacterium* species, as such being the antibiotic of choice prescribed against tuberculosis [81, 82]. Hence, in the context of our study, these antibiotics would be ineffective against *P. agglomerans* KM1 strain. Previous studies showed that isolates of *P. agglomerans* harbored wide spectrum of antibiotic resistant genes, clinical reports demonstrated cases of pneumonia and death in children with comorbidities where the causative agent was identified as a carbapenem-resistant *P. agglomerans* [12]. Additionally, another study showed that fifty percent of *P. agglomerans* isolates extracted from an infant formula milk were resistant to cefotaxime, moxifloxacin, cotrimoxazole and ticarcillin [10]. As such, the food-borne *P. agglomerans*, including the KM1 isolate, may serve as reservoir of antibiotic resistance genes, posing health risks, food safety concerns, and contributing to the spread of antibiotic resistance through horizontal gene transfer. These findings suggest that *P. agglomerans* may increasingly become more common in clinical settings, as reported in case of major nosocomial pathogens such as *Acinetobacter baumannii* and *Pseudomonas aeruginosa* [83].

Interestingly, the same virulence factors of KM1 strain were found back in the closely related complete genomes of *P. agglomerans* strains L15, TH81, UAEU18 and C410P1. For *P. agglomerans* Tx10, a clinical isolate from the sputum sample of a cystic fibrosis patient, similar virulence factors of KM1 can be found in the NCBI database despite the incomplete deposition of the genome sequence of this strain [84]. The *P. agglomerans* pan-genome analysis of various soil and plant derived isolates as well as a clinical sample, revealed the presence of multiple antibiotic resistance genes and virulence factors, including genes related to T6SS effectors, iron uptake system, adhesion, hemolysin and flagella. Notably, genes related to type III secretion system (T3SS), which are genotypic trait of phytopathogenic *P. agglomerans*, were absent in the KM1 strain [85]. These virulence genes in *P. agglomerans* may play a role in niche-adaptation, colonization and pathogenesis in a wide range of hosts.

In order to complete the characterization of isolated *P. agglomerans* KM1, immunostimulatory properties were assessed, using RAW 264.7 macrophages. The heat inactivated whole-cell preparation of *P. agglomerans* triggered secretion of pro-inflammatory cytokines TNF-α and IL-6, as well as NO. At the same time, culture supernatants contained high levels of anti-inflammatory IL-10. While the bacterial cell wall contains lipopolisacharide (LPS), the main immuno-stimulatory molecule and a well-known agonist of TLR4, bacterial triacylated lipoproteins were shown to activate TLR1/2 signaling pathway [86, 87]. Previously published reports attributed TNF-α production mainly to the action of *P. agglomerans* derived LPS, able to trigger activation of the TLR4. Our current study provides an additional evidence that beside the strong involvement of the TLR4, TNF-α section can also be mediated by TLR1/2, however to a lesser extent. The analysis of the downstream involvement of transcriptional factors such as NF-kB or MAPKKs in TNF-α secretion indicated dominant activation of NF-kB and no activation of MAPKKs (86–88]. The dependence on the NF-κB was also demonstrated in case of secretion of IL-6 and NO. Here in contrast to TNF-α, a strong involvement of both TLR1/2 and TLR4 was recorded. Interestingly, the heat inactivated whole-cell preparation of *P. agglomerans* was also capable of inducting IL-10 production. The anti-inflammatory cytokine IL-10 was shown to antagonize the action of pro-inflammatory cytokines such as TNF-α, preventing tissue and cell injury due to induction of an excessive inflammation with cytotoxic activity [88]. The secretion of IL-10 was mainly dependent on TLR4 and to a lesser extent on TLR1/2 signaling. While the role of TLR2 in section of IL-10 is well documented, the involvement of the TLR4 is less characterized, and as such our study sheds a new light on TLR4 mediated IL-10 secretion [89–92]. Important to keep in mind is that the abrogation of IL-10 secretion may reflect a cumulative effect of the deletion of the TLR4 present on the surface and

TLR4 located in endosomal compartment. As opposed to production of TNF-α, Il-6 and NO production, the secretion of IL-10 involved partial activation of MAPKKs and the dominant role of the NF-κB. The involvement of TLR4 in signaling for IL-10 secretion may have an additional regulatory function in maintaining the balance between secretion of the pro-inflammatory and inflammatory cytokines, controlling at the same time the extent of an injury during inflammation.

In conclusion, the genome analysis of the foodborne isolate *P. agglomerans* KM1 improves our understanding of its virulence determinants indicating potential for pathogenicity. In addition to thirteen antibiotic resistance genes, several virulence factors were identified such as the complete T6SS, filamentous hemagglutinin, siderophore-mediated iron acquisition system (Enterobactin transporter) and hemolysin. The KM1 strain showed strong immuno-stimulatory properties on RAW 264.7 macrophages, with a dominant role of TLR4 signaling and NF-κB activation, resulting in secretion of TNF-α, Il-6, NO and Il-10. Further large-scale studies of clinical isolates are needed to validate the identified virulence factors and antibiotic resistance genes of this potentially opportunistic *P. agglomerans*. Hence, the high quality draft genome of *P. agglomerans* KM1 will provide a baseline for further studies leading to in-depth understanding of molecular mechanisms of *P. agglomerans* pathogenesis.

Supporting information

S1 Fig. Assessment of the completeness of genome assembly and annotation of *P. agglomerans* KM1 using BUSCO. Colors refer to the percentage of the complete single-copy orthologs (light blue), complete duplicated orthologs (blue), fragmented or incomplete orthologs (yellow), and missing orthologs (red).
(DOCX)

S2 Fig. Subsystem category distribution of *P. agglomerans* KM1 genome based on the SEED database. Bar chart shows the percentage of subsystem coverage with green bar corresponding to the percentage of proteins involved. The pie chart shows the distribution and count of each SEED subsystem feature.
(DOCX)

S3 Fig. Core and pan-genome analysis of five *P. agglomerans* strains. (A) Heap's law chart representation regarding conserved genes and total genes in *P. agglomerans* genomes. (B) Diagram of new genes vs. unique genes in relation to number of genomes embedded in the analysis.
(DOCX)

S4 Fig. Linear genomic map of *P. agglomerans* KM1 phage-associated regions obtained with PHASTER. Different functional groups of coding sequences of phage origins are denoted by different colors, according to their function.
(DOCX)

S5 Fig. Gel electrophoresis of amplified PCR products of type VI secretion system in *P. agglomerans* KM1. Lane 1: 100 bp DNA marker, Lane 2: *Hcp* negative control, Lane 3: *Hcp* in KM1, Lane 4: *VgrG* negative control, Lane 5: *VgrG* in KM1. The amplicon size of T6SS effectors were 1301 bp (*Hcp)* and 1011 bp (*VgrG*).
(DOCX)

S1 Table. Genomic islands present in the *P. agglomerans* KM1.
(XLS)

S2 Table. CRISPR loci of *P. agglomerans* KM1.
(XLSX)

S3 Table. Biochemical identification of *P. agglomerans* KM1 using API 20E test kit.
(DOCX)

S4 Table. Genotypic antibiotic resistance gene profile of *P. agglomerans* KM1.
(DOCX)

Acknowledgments

Preliminary experiments preceding the results presented in this paper were technically executed in part by Miss K. Arora, Miss M. Kim and Mr. N. Vereecke, former members of the laboratory assistant team at Ghent University Global Campus.

Author Contributions

Conceptualization: Robin B. Guevarra, Stefan Magez, Eveline Peeters, Mi Sook Chung, Kyung Hyun Kim, Magdalena Radwanska.

Formal analysis: Robin B. Guevarra, Stefan Magez, Magdalena Radwanska.

Funding acquisition: Magdalena Radwanska.

Investigation: Stefan Magez, Eveline Peeters, Magdalena Radwanska.

Methodology: Robin B. Guevarra, Stefan Magez, Magdalena Radwanska.

Project administration: Magdalena Radwanska.

Resources: Mi Sook Chung, Kyung Hyun Kim, Magdalena Radwanska.

Supervision: Stefan Magez, Magdalena Radwanska.

Visualization: Robin B. Guevarra, Stefan Magez.

Writing – original draft: Robin B. Guevarra, Stefan Magez, Magdalena Radwanska.

Writing – review & editing: Robin B. Guevarra, Stefan Magez, Eveline Peeters, Mi Sook Chung, Kyung Hyun Kim, Magdalena Radwanska.

References

1. Park KY, Jeong JK, Lee YE, Daily JW 3rd. Health benefits of kimchi (Korean fermented vegetables) as a probiotic food. Journal of medicinal food. 2014; 17(1):6–20. https://doi.org/10.1089/jmf.2013.3083 PMID: 24456350
2. Patra JK, Das G, Paramithiotis S, Shin HS. Kimchi and other widely consumed traditional fermented foods of Korea: A review. Frontiers in microbiology. 2016; 7:1493. https://doi.org/10.3389/fmicb.2016.01493 PMID: 27733844
3. Jung JY, Lee SH, Kim JM, Park MS, Bae JW, Hahn Y, et al. Metagenomic analysis of kimchi, a traditional Korean fermented food. Applied and environmental microbiology. 2011; 77(7):2264–74. https://doi.org/10.1128/AEM.02157-10 PMID: 21317261
4. Song WJ, Chung HY, Kang DH, Ha JW. Microbial quality of reduced-sodium napa cabbage kimchi and its processing. Food science & nutrition. 2019; 7(2):628–35. https://doi.org/10.1002/fsn3.898 PMID: 30847142
5. Shin J, Yoon KB, Jeon DY, Oh SS, Oh KH, Chung GT, et al. Consecutive outbreaks of Enterotoxigenic *Escherichia coli* O6 in schools in South Korea caused by contamination of fermented vegetable kimchi. Foodborne pathogens and disease. 2016; 13(10):535–43. https://doi.org/10.1089/fpd.2016.2147 PMID: 27557346

6. Choi Y, Lee S, Kim HJ, Lee H, Kim S, Lee J, et al. Pathogenic *Escherichia coli* and *Salmonella* can survive in kimchi during fermentation. Journal of food protection. 2018; 81(6):942–6. https://doi.org/10.4315/0362-028X.JFP-17-459 PMID: 29745760

7. Luziatelli F, Ficca AG, Melini F, Ruzzi M. Genome sequence of the plant growth-promoting rhizobacterium *Pantoea agglomerans* C1. Microbiology resource announcements. 2019; 8(44). https://doi.org/10.1128/MRA.00828-19 PMID: 31672740

8. Humphrey J, Seitz T, Haan T, Ducluzeau AL, Drown DM. Complete genome sequence of *Pantoea agglomerans* TH81, isolated from a permafrost thaw gradient. Microbiology resource announcements. 2019; 8(1). https://doi.org/10.1128/MRA.01486-18 PMID: 30637402

9. Palmer M, de Maayer P, Poulsen M, Steenkamp ET, van Zyl E, Coutinho TA, et al. Draft genome sequences of *Pantoea agglomerans* and *Pantoea vagans* isolates associated with termites. Standards in genomic sciences. 2016; 11:23. https://doi.org/10.1186/s40793-016-0144-z PMID: 26937267

10. Mardaneh J, Dallal MM. Isolation, identification and antimicrobial susceptibility of Pantoea (*Enterobacter*) *agglomerans* isolated from consumed powdered infant formula milk (PIF) in NICU ward: First report from Iran. Iranian journal of microbiology. 2013; 5(3):263–7. PMID: 24475334

11. De Champs C, Le Seaux S, Dubost JJ, Boisgard S, Sauvezie B, Sirot J. Isolation of *Pantoea agglomerans* in two cases of septic monoarthritis after plant thorn and wood sliver injuries. Journal of clinical microbiology. 2000; 38(1):460–1. PMID: 10618144

12. Buyukcam A, Tuncer O, Gur D, Sancak B, Ceyhan M, Cengiz AB, et al. Clinical and microbiological characteristics of *Pantoea agglomerans* infection in children. Journal of infection and public health. 2018; 11(3):304–9. https://doi.org/10.1016/j.jiph.2017.07.020 PMID: 28780309

13. Cruz AT, Cazacu AC, Allen CH. *Pantoea agglomerans*, a plant pathogen causing human disease. Journal of clinical microbiology. 2007; 45(6):1989–92. https://doi.org/10.1128/JCM.00632-07 PMID: 17442803

14. Walterson AM, Stavrinides J. *Pantoea*: insights into a highly versatile and diverse genus within the Enterobacteriaceae. FEMS microbiology reviews. 2015; 39(6):968–84. https://doi.org/10.1093/femsre/fuv027 PMID: 26109597

15. Lim JA, Lee DH, Kim BY, Heu S. Draft genome sequence of *Pantoea agglomerans* R190, a producer of antibiotics against phytopathogens and foodborne pathogens. Journal of biotechnology. 2014; 188:7–8. https://doi.org/10.1016/j.jbiotec.2014.07.440 PMID: 25087741

16. Pusey PL, Stockwell VO, Reardon CL, Smits TH, Duffy B. Antibiosis activity of *Pantoea agglomerans* biocontrol strain E325 against *Erwinia amylovora* on apple flower stigmas. Phytopathology. 2011; 101 (10):1234–41. https://doi.org/10.1094/PHYTO-09-10-0253 PMID: 21679036

17. Shariati JV, Malboobi MA, Tabrizi Z, Tavakol E, Owilia P, Safari M. Comprehensive genomic analysis of a plant growth-promoting rhizobacterium *Pantoea agglomerans* strain P5. Scientific reports. 2017; 7 (1):15610. https://doi.org/10.1038/s41598-017-15820-9 PMID: 29142289

18. Smits TH, Rezzonico F, Kamber T, Blom J, Goesmann A, Ishimaru CA, et al. Metabolic versatility and antibacterial metabolite biosynthesis are distinguishing genomic features of the fire blight antagonist *Pantoea vagans* C9-1. PloS one. 2011; 6(7):e22247. https://doi.org/10.1371/journal.pone.0022247 PMID: 21789243

19. Fukasaka M, Asari D, Kiyotoh E, Okazaki A, Gomi Y, Tanimoto T, et al. A lipopolysaccharide from *Pantoea agglomerans* is a promising adjuvant for sublingual vaccines to induce systemic and mucosal immune responses in mice via TLR4 pathway. PloS one. 2015; 10(5):e0126849. https://doi.org/10.1371/journal.pone.0126849 PMID: 25978818

20. Hebishima T, Matsumoto Y, Watanabe G, Soma G, Kohchi C, Taya K, et al. Oral administration of immunopotentiator from *Pantoea agglomerans* 1 (IP-PA1) improves the survival of B16 melanoma-inoculated model mice. Experimental animals. 2011; 60(2):101–9. https://doi.org/10.1538/expanim.60.101 PMID: 21512265

21. Kobayashi Y, Inagawa H, Kohchi C, Kazumura K, Tsuchiya H, Miwa T, et al. Oral administration of *Pantoea agglomerans*-derived lipopolysaccharide prevents development of atherosclerosis in high-fat diet-fed apoE-deficient mice via ameliorating hyperlipidemia, pro-inflammatory mediators and oxidative responses. PloS one. 2018; 13(3):e0195008. https://doi.org/10.1371/journal.pone.0195008 PMID: 29584779

22. Dutkiewicz J, Mackiewicz B, Lemieszek MK, Golec M, Milanowski J. *Pantoea agglomerans*: a marvelous bacterium of evil and good.Part I. Deleterious effects: Dust-borne endotoxins and allergens—focus on cotton dust. Annals of agricultural and environmental medicine: AAEM. 2015; 22(4):576–88. https://doi.org/10.5604/12321966.1185757 PMID: 26706959

23. Dutkiewicz J, Mackiewicz B, Kinga Lemieszek M, Golec M, Milanowski J. *Pantoea agglomerans*: a mysterious bacterium of evil and good. Part III. Deleterious effects: infections of humans, animals and

plants. Annals of agricultural and environmental medicine: AAEM. 2016; 23(2):197–205. https://doi.org/10.5604/12321966.1203878 PMID: 27294620

24. Tiwari S, Beriha SS. *Pantoea* species causing early onset neonatal sepsis: a case report. Journal of medical case reports. 2015; 9:188. https://doi.org/10.1186/s13256-015-0670-0 PMID: 26341678
25. Yablon BR, Dantes R, Tsai V, Lim R, Moulton-Meissner H, Arduino M, et al. Outbreak of Pantoea agglomerans Bloodstream Infections at an Oncology Clinic-Illinois, 2012–2013. Infection control and hospital epidemiology. 2017; 38(3):314–9.
26. Dutkiewicz J, Mackiewicz B, Lemieszek MK, Golec M, Skorska C, Gora-Florek A, et al. *Pantoea agglomerans*: a mysterious bacterium of evil and good. Part II—Deleterious effects: Dust-borne endotoxins and allergens—focus on grain dust, other agricultural dusts and wood dust. Annals of agricultural and environmental medicine: AAEM. 2016; 23(1):6–29. https://doi.org/10.5604/12321966.1196848 PMID: 27007514
27. Mackiewicz B, Dutkiewicz J, Siwiec J, Kucharczyk T, Siek E, Wojcik-Fatla A, et al. Acute hypersensitivity pneumonitis in woodworkers caused by inhalation of birch dust contaminated with *Pantoea agglomerans* and *Microbacterium barkeri*. Annals of agricultural and environmental medicine: AAEM. 2019; 26 (4):644–55. https://doi.org/10.26444/aaem/114931 PMID: 31885240
28. Milanowski J, Dutkiewicz J. Increased superoxide anion generation by alveolar macrophages stimulated with antigens associated with organic dusts. Allergologia et immunopathologia. 1990; 18(4):211–5. PMID: 2176060
29. Mudryk M. *Plant-isolated Pantoea agglomerans*—new look into potential pathogenicity. Mikrobiolohichnyi zhurnal. 2012; 74(6):53–7. PMID: 23293827
30. Moghadam F, Couger MB, Russ B, Ramsey R, Hanafy RA, Budd C, et al. Draft genome sequence and detailed analysis of *Pantoea eucrina* strain *Russ* and implication for opportunistic pathogenesis. Genomics data. 2016; 10:63–8. https://doi.org/10.1016/j.gdata.2016.09.006 PMID: 27699151
31. Bankevich A, Nurk S, Antipov D, Gurevich AA, Dvorkin M, Kulikov AS, et al. SPAdes: a new genome assembly algorithm and its applications to single-cell sequencing. Journal of computational biology: a journal of computational molecular cell biology. 2012; 19(5):455–77. https://doi.org/10.1089/cmb.2012.0021 PMID: 22506599
32. Walker BJ, Abeel T, Shea T, Priest M, Abouelliel A, Sakthikumar S, et al. Pilon: an integrated tool for comprehensive microbial variant detection and genome assembly improvement. PloS one. 2014; 9(11): e112963. https://doi.org/10.1371/journal.pone.0112963 PMID: 25409509
33. Wick RR, Schultz MB, Zobel J, Holt KE. Bandage: interactive visualization of de novo genome assemblies. Bioinformatics. 2015; 31(20):3350–2. https://doi.org/10.1093/bioinformatics/btv383 PMID: 26099265
34. Gurevich A, Saveliev V, Vyahhi N, Tesler G. QUAST: quality assessment tool for genome assemblies. Bioinformatics. 2013; 29(8):1072–5. https://doi.org/10.1093/bioinformatics/btt086 PMID: 23422339
35. Simao FA, Waterhouse RM, Ioannidis P, Kriventseva EV, Zdobnov EM. BUSCO: assessing genome assembly and annotation completeness with single-copy orthologs. Bioinformatics. 2015; 31(19):3210–2. https://doi.org/10.1093/bioinformatics/btv351 PMID: 26059717
36. Tatusova T, DiCuccio M, Badretdin A, Chetvernin V, Nawrocki EP, Zaslavsky L, et al. NCBI prokaryotic genome annotation pipeline. Nucleic acids research. 2016; 44(14):6614–24. https://doi.org/10.1093/nar/gkw569 PMID: 27342282
37. Lowe TM, Eddy SR. tRNAscan-SE: a program for improved detection of transfer RNA genes in genomic sequence. Nucleic acids research. 1997; 25(5):955–64. https://doi.org/10.1093/nar/25.5.955 PMID: 9023104
38. Lagesen K, Hallin P, Rodland EA, Staerfeldt HH, Rognes T, Ussery DW. RNAmmer: consistent and rapid annotation of ribosomal RNA genes. Nucleic acids research. 2007; 35(9):3100–8. https://doi.org/10.1093/nar/gkm160 PMID: 17452365
39. Wu S, Zhu Z, Fu L, Niu B, Li W. WebMGA: a customizable web server for fast metagenomic sequence analysis. BMC genomics. 2011; 12:444. https://doi.org/10.1186/1471-2164-12-444 PMID: 21899761
40. Aziz RK, Bartels D, Best AA, DeJongh M, Disz T, Edwards RA, et al. The RAST Server: rapid annotations using subsystems technology. BMC genomics. 2008; 9:75. https://doi.org/10.1186/1471-2164-9-75 PMID: 18261238
41. Petkau A, Stuart-Edwards M, Stothard P, Van Domselaar G. Interactive microbial genome visualization with GView. Bioinformatics. 2010; 26(24):3125–6. https://doi.org/10.1093/bioinformatics/btq588 PMID: 20956244
42. Yoon SH, Ha SM, Kwon S, Lim J, Kim Y, Seo H, et al. Introducing EzBioCloud: a taxonomically united database of 16S rRNA gene sequences and whole-genome assemblies. International journal of

systematic and evolutionary microbiology. 2017; 67(5):1613–7. https://doi.org/10.1099/ijsem.0.001755 PMID: 28005526

43. Deletoile A, Decre D, Courant S, Passet V, Audo J, Grimont P, et al. Phylogeny and identification of *Pantoea* species and typing of *Pantoea agglomerans* strains by multilocus gene sequencing. Journal of clinical microbiology. 2009; 47(2):300–10. https://doi.org/10.1128/JCM.01916-08 PMID: 19052179

44. Kumar S, Stecher G, Li M, Knyaz C, Tamura K. MEGA X: Molecular Evolutionary Genetics Analysis across computing platforms. Molecular biology and evolution. 2018; 35(6):1547–9. https://doi.org/10.1093/molbev/msy096 PMID: 29722887

45. Darling AC, Mau B, Blattner FR, Perna NT. Mauve: multiple alignment of conserved genomic sequence with rearrangements. Genome research. 2004; 14(7):1394–403. https://doi.org/10.1101/gr.2289704 PMID: 15231754

46. Seemann T. Prokka: rapid prokaryotic genome annotation. Bioinformatics. 2014; 30(14):2068–9. https://doi.org/10.1093/bioinformatics/btu153 PMID: 24642063

47. Page AJ, Cummins CA, Hunt M, Wong VK, Reuter S, Holden MT, et al. Roary: rapid large-scale prokaryote pan genome analysis. Bioinformatics. 2015; 31(22):3691–3. https://doi.org/10.1093/bioinformatics/btv421 PMID: 26198102

48. Bertelli C, Laird MR, Williams KP, Simon Fraser University Research Computing G, Lau BY, Hoad G, et al. IslandViewer 4: expanded prediction of genomic islands for larger-scale datasets. Nucleic acids research. 2017; 45(W1):W30–W5. https://doi.org/10.1093/nar/gkx343 PMID: 28472413

49. Arndt D, Grant JR, Marcu A, Sajed T, Pon A, Liang Y, et al. PHASTER: a better, faster version of the PHAST phage search tool. Nucleic acids research. 2016; 44(W1):W16–21. https://doi.org/10.1093/nar/gkw387 PMID: 27141966

50. Grissa I, Vergnaud G, Pourcel C. CRISPRFinder: a web tool to identify clustered regularly interspaced short palindromic repeats. Nucleic acids research. 2007; 35(Web Server issue):W52–7. https://doi.org/10.1093/nar/gkm360 PMID: 17537822

51. McArthur AG, Waglechner N, Nizam F, Yan A, Azad MA, Baylay AJ, et al. The comprehensive antibiotic resistance database. Antimicrobial agents and chemotherapy. 2013; 57(7):3348–57. https://doi.org/10.1128/AAC.00419-13 PMID: 23650175

52. Chen L, Yang J, Yu J, Yao Z, Sun L, Shen Y, et al. VFDB: a reference database for bacterial virulence factors. Nucleic acids research. 2005; 33(Database issue):D325–8. https://doi.org/10.1093/nar/gki008 PMID: 15608208

53. Zhang Y, Yan H, Lu W, Li Y, Guo X, Xu B. A novel Omega-class glutathione S-transferase gene in *Apis cerana cerana*: molecular characterisation of GSTO2 and its protective effects in oxidative stress. Cell stress & chaperones. 2013; 18(4):503–16. https://doi.org/10.1007/s12192-013-0406-2 PMID: 23382010

54. Bible AN, Fletcher SJ, Pelletier DA, Schadt CW, Jawdy SS, Weston DJ, et al. A carotenoid-deficient mutant in *Pantoea* sp. YR343, a bacteria isolated from the rhizosphere of *Populus deltoides*, is defective in root colonization. Frontiers in microbiology. 2016; 7:491. https://doi.org/10.3389/fmicb.2016.00491 PMID: 27148182

55. Costa E, Usall J, Teixido N, Delgado J, Vinas I. Water activity, temperature, and pH effects on growth of the biocontrol agent *Pantoea agglomerans* CPA-2. Canadian journal of microbiology. 2002; 48(12):1082–8. https://doi.org/10.1139/w03-001 PMID: 12619821

56. Teixido N, Canamas TP, Abadias M, Usall J, Solsona C, Casals C, et al. Improving low water activity and desiccation tolerance of the biocontrol agent *Pantoea agglomerans* CPA-2 by osmotic treatments. Journal of applied microbiology. 2006; 101(4):927–37. https://doi.org/10.1111/j.1365-2672.2006.02948.x PMID: 16968304

57. Haiko J, Westerlund-Wikstrom B. The role of the bacterial flagellum in adhesion and virulence. Biology. 2013; 2(4):1242–67. https://doi.org/10.3390/biology2041242 PMID: 24833223

58. Rouli L, Merhej V, Fournier PE, Raoult D. The bacterial pangenome as a new tool for analysing pathogenic bacteria. New microbes and new infections. 2015; 7:72–85. https://doi.org/10.1016/j.nmni.2015.06.005 PMID: 26442149

59. Kim D, Hong S, Kim YT, Ryu S, Kim HB, Lee JH. Metagenomic approach to identifying foodborne pathogens on Chinese cabbage. Journal of microbiology and biotechnology. 2018; 28(2):227–35. https://doi.org/10.4014/jmb.1710.10021 PMID: 29169222

60. Oie S, Kiyonaga H, Matsuzaka Y, Maeda K, Masuda Y, Tasaka K, et al. Microbial contamination of fruit and vegetables and their disinfection. Biological & pharmaceutical bulletin. 2008; 31(10):1902–5. https://doi.org/10.1248/bpb.31.1902 PMID: 18827352

61. Mougous JD, Cuff ME, Raunser S, Shen A, Zhou M, Gifford CA, et al. A virulence locus of *Pseudomonas aeruginosa* encodes a protein secretion apparatus. Science. 2006; 312(5779):1526–30. https://doi.org/10.1126/science.1128393 PMID: 16763151

62. Pukatzki S, Ma AT, Sturtevant D, Krastins B, Sarracino D, Nelson WC, et al. Identification of a conserved bacterial protein secretion system in *Vibrio cholerae* using the *Dictyostelium* host model system. Proceedings of the National Academy of Sciences of the United States of America. 2006; 103(5):1528–33. https://doi.org/10.1073/pnas.0510322103 PMID: 16432199

63. Cianfanelli FR, Alcoforado Diniz J, Guo M, De Cesare V, Trost M, Coulthurst SJ. VgrG and PAAR proteins define distinct versions of a functional type VI secretion system. PLoS pathogens. 2016; 12(6): e1005735. https://doi.org/10.1371/journal.ppat.1005735 PMID: 27352036

64. Pukatzki S, McAuley SB, Miyata ST. The type VI secretion system: translocation of effectors and effector-domains. Current opinion in microbiology. 2009; 12(1):11–7. https://doi.org/10.1016/j.mib.2008.11.010 PMID: 19162533

65. Ho BT, Dong TG, Mekalanos JJ. A view to a kill: the bacterial type VI secretion system. Cell host & microbe. 2014; 15(1):9–21. https://doi.org/10.1016/j.chom.2013.11.008 PMID: 24332978

66. Shyntum DY, Venter SN, Moleleki LN, Toth I, Coutinho TA. Comparative genomics of type VI secretion systems in strains of *Pantoea ananatis* from different environments. BMC genomics. 2014; 15:163. https://doi.org/10.1186/1471-2164-15-163 PMID: 24571088

67. Clemens DL, Lee BY, Horwitz MA. The *Francisella* type VI secretion system. Frontiers in cellular and infection microbiology. 2018; 8:121. https://doi.org/10.3389/fcimb.2018.00121 PMID: 29740542

68. Inatsuka CS, Julio SM, Cotter PA. *Bordetella* filamentous hemagglutinin plays a critical role in immunomodulation, suggesting a mechanism for host specificity. Proceedings of the National Academy of Sciences of the United States of America. 2005; 102(51):18578–83. https://doi.org/10.1073/pnas.0507910102 PMID: 16339899

69. Locht C, Bertin P, Menozzi FD, Renauld G. The filamentous haemagglutinin, a multifaceted adhesion produced by virulent *Bordetella* spp. Molecular microbiology. 1993; 9(4):653–60. https://doi.org/10.1111/j.1365-2958.1993.tb01725.x PMID: 8231801

70. Confer AW, Ayalew S. The OmpA family of proteins: roles in bacterial pathogenesis and immunity. Veterinary microbiology. 2013; 163(3–4):207–22. https://doi.org/10.1016/j.vetmic.2012.08.019 PMID: 22986056

71. Vandenesch F, Lina G, Henry T. *Staphylococcus aureus* hemolysins, bi-component leukocidins, and cytolytic peptides: a redundant arsenal of membrane-damaging virulence factors? Frontiers in cellular and infection microbiology. 2012; 2:12. https://doi.org/10.3389/fcimb.2012.00012 PMID: 22919604

72. Krewulak KD, Vogel HJ. Structural biology of bacterial iron uptake. Biochimica et biophysica acta. 2008; 1778(9):1781–804. https://doi.org/10.1016/j.bbamem.2007.07.026 PMID: 17916327

73. Andrews SC, Robinson AK, Rodriguez-Quinones F. Bacterial iron homeostasis. FEMS microbiology reviews. 2003; 27(2–3):215–37. https://doi.org/10.1016/S0168-6445(03)00055-X PMID: 12829269

74. Guo Y, Hu D, Guo J, Li X, Guo J, Wang X, et al. The role of the regulator *Fur* in gene regulation and virulence of *Riemerella anatipestifer* assessed using an unmarked gene deletion system. Frontiers in cellular and infection microbiology. 2017; 7:382. https://doi.org/10.3389/fcimb.2017.00382 PMID: 28971067

75. Aly MA, Domig KJ, Kneifel W, Reimhult E. Whole genome sequencing-based comparison of food isolates of *Cronobacter sakazakii*. Frontiers in microbiology. 2019; 10:1464. https://doi.org/10.3389/fmicb.2019.01464 PMID: 31333604

76. Su M, Satola SW, Read TD. Genome-based prediction of bacterial antibiotic resistance. Journal of clinical microbiology. 2019; 57(3). https://doi.org/10.1128/JCM.01405-18 PMID: 30381421

77. Siwakoti S, Sah R, Rajbhandari RS, Khanal B. *Pantoea agglomerans* infections in children: Report of two cases. Case reports in pediatrics. 2018; 2018:4158734. https://doi.org/10.1155/2018/4158734 PMID: 29527373

78. Nguyen R, Khanna NR, Sun Y. Bacitracin topical. StatPearls. Treasure Island (FL)2020.

79. Bonomo RA, Van Zile PS, Li Q, Shermock KM, McCormick WG, Kohut B. Topical triple-antibiotic ointment as a novel therapeutic choice in wound management and infection prevention: a practical perspective. Expert review of anti-infective therapy. 2007; 5(5):773–82. https://doi.org/10.1586/14787210.5.5.773 PMID: 17914912

80. Gardiner BJ, Stewardson AJ, Abbott IJ, Peleg AY. Nitrofurantoin and fosfomycin for resistant urinary tract infections: old drugs for emerging problems. Australian prescriber. 2019; 42(1):14–9. https://doi.org/10.18773/austprescr.2019.002 PMID: 30765904

81. Hawley HB, Gump DW. Vancomycin therapy of bacterial meningitis. American journal of diseases of children. 1973; 126(2):261–4. https://doi.org/10.1001/archpedi.1973.02110190231025 PMID: 4724121

82. Alifano P, Palumbo C, Pasanisi D, Tala A. Rifampicin-resistance, rpoB polymorphism and RNA polymerase genetic engineering. Journal of biotechnology. 2015; 202:60–77. https://doi.org/10.1016/j.jbiotec.2014.11.024 PMID: 25481100

83. Zavascki AP, Carvalhaes CG, Picao RC, Gales AC. Multidrug-resistant *Pseudomonas aeruginosa* and *Acinetobacter baumannii*: resistance mechanisms and implications for therapy. Expert review of anti-infective therapy. 2010; 8(1):71–93. https://doi.org/10.1586/eri.09.108 PMID: 20014903

84. Smith DD, Kirzinger MW, Stavrinides J. Draft genome sequence of the antibiotic-producing cystic fibrosis isolate *Pantoea agglomerans* Tx10. Genome announcements. 2013; 1(5). https://doi.org/10.1128/genomeA.00904-13 PMID: 24179115

85. Rezzonico F, Smits TH, Montesinos E, Frey JE, Duffy B. Genotypic comparison of *Pantoea agglomerans* plant and clinical strains. BMC microbiology. 2009; 9:204. https://doi.org/10.1186/1471-2180-9-204 PMID: 19772624

86. Irvine KL, Hopkins LJ, Gangloff M, Bryant CE. The molecular basis for recognition of bacterial ligands at equine TLR2, TLR1 and TLR6. Veterinary research. 2013; 44:50. https://doi.org/10.1186/1297-9716-44-50 PMID: 23826682

87. Takeda K, Akira S. Toll-like receptors. Current protocols in immunology. 2015; 109:14 2 1–2 0. https://doi.org/10.1002/0471142735.im1412s109 PMID: 25845562

88. Couper KN, Blount DG, Riley EM. IL-10: the master regulator of immunity to infection. Journal of immunology. 2008; 180(9):5771–7. https://doi.org/10.4049/jimmunol.180.9.5771 PMID: 18424693

89. Li J, Lee DS, Madrenas J. Evolving bacterial envelopes and plasticity of TLR2-dependent responses: Basic research and translational opportunities. Frontiers in immunology. 2013; 4:347. https://doi.org/10.3389/fimmu.2013.00347 PMID: 24191155

90. Morrison DK. MAP kinase pathways. Cold Spring Harbor perspectives in biology. 2012; 4(11). https://doi.org/10.1101/cshperspect.a011254 PMID: 23125017

91. Hu X, Paik PK, Chen J, Yarilina A, Kockeritz L, Lu TT, et al. IFN-gamma suppresses IL-10 production and synergizes with TLR2 by regulating GSK3 and CREB/AP-1 proteins. Immunity. 2006; 24(5):563–74. https://doi.org/10.1016/j.immuni.2006.02.014 PMID: 16713974

92. Sanin DE, Prendergast CT, Mountford AP. IL-10 Production in macrophages is regulated by a TLR-driven CREB-mediated mechanism that is linked to genes involved in cell metabolism. Journal of immunology. 2015; 195(3):1218–32. https://doi.org/10.4049/jimmunol.1500146 PMID: 26116503